mathematics

MDPI

Article

Joint Optimization of Multi-Cycle Timetable Considering Supply-to-Demand Relationship and Energy Consumption for Rail Express

Han Zheng, Junhua Chen *, Zhaocha Huang and Jianhao Zhu

School of Traffic and Transportation, Beijing Jiaotong University, No. 3 Shang Yuan Cun, Hai Dian District, Beijing 100044, China
* Correspondence: cjh@bjtu.edu.cn

Abstract: Rail expresses play a vital role in intracity and intercity transportations. For accommodating multi-source passenger traffic with different travel demand, while optimizing the energy consumption, we propose a multi-cycle train timetable optimization model and a decomposition algorithm. A periodized spatial-temporal network that can support the integrated optimization of passenger service satisfaction and energy consumption considering multi-cycles is studied as the basis of the modeling. Based on this, an integrated optimization model taking the planning of the train spatial-temporal path, cycle length and active lines as variables is proposed. Then, for solving the issues caused by the complex relationships among the cycle length, line and train spatial-temporal path in large-scale cases, a hybrid heuristic Lagrangian decomposition method is investigated. Numerical experiments under different passenger flow demand scenarios are performed. The results show that the more fluctuating the passenger flow is, the more obvious the advantage of a multi-cycle timetable is. For the scenario with two passenger flow peaks, compared to a single-cycle timetable, the demand satisfaction ratio of the multi-cycle timetable is 4.44% higher and the train vacancy rate is 11.49% lower. A multi-cycle timetable also saves 3.24 h running time and 15,553.6 kwh energy consumption compared to a single-cycle timetable. Large-scale real cases show that this advantage still exists in practice.

Keywords: rail express; passenger flow demand; multi-cycle train timetable; energy consumption; spatial-temporal network; Lagrangian relaxation

MSC: 90B06

Citation: Zheng, H.; Chen, J.; Huang, Z.; Zhu, J. Joint Optimization of Multi-Cycle Timetable Considering Supply-to-Demand Relationship and Energy Consumption for Rail Express. *Mathematics* **2022**, *10*, 4164. https://doi.org/10.3390/math10214164

Academic Editor: Ripon Kumar Chakrabortty

Received: 25 September 2022
Accepted: 4 November 2022
Published: 7 November 2022

1. Introduction

1.1. Background

Along with the continuous urbanization and growth of the city scale, the functional positionings of different areas in a city are gradually being clarified and the relationships between such areas are more diverse. This leads to a much more complex passenger traveling demand. Multi-source passenger flows generated from different areas, such as tourism, business, commuting, schooling, etc., have individual travel times, frequencies and their own time peaks. Aggregated along the time dimension, the overall flow unveils unique characteristics, such as a wide peak, single peak or multi-peaks. At the same time, green transportation is also one of the important directions of urban development. Thus, for rail express operators, train schedules need to not only meet the demand–supply relationships but also optimize the operating costs and energy consumption.

For meeting the demand–supply relationships, the plan should not only be flexible to adapt to the characteristics of passenger demand but also be formulated as a regular and easy-to-memorize schedule. Moreover, the model should consider and optimize the energy consumption of the train fleet. A multi-cycle timetable, which is composed of a set

of running lines with different frequencies and period lengths, is a good choice to meet such requirements. Compared with the single-cycle train timetable, the multi-cycle train timetable ensures the regularity and satisfies the passenger demand of different periods by flexibly arranging the train departure time and the cycle length. Thus, it is necessary to develop a multi-cycle train timetable that can accommodate the peaks caused by the multi-source passenger demand while considering a proper combination of trains with different stopping patterns and cycle lengths for better energy consumption.

There exists a relationship between the energy consumption and passenger demand satisfaction. The train stops at different stations to provide transportation services, which will affect the service satisfaction of passengers. Such kinds of stoppings are determined by the line planning. In addition, trains of different speed classes will have crossings due to the space–time relationship, thus leading to additional stoppings. Such kinds of stoppings are determined by the train diagram (i.e., timetable). Train stopping is unavoidably accompanied by train deceleration and acceleration, which directly affects the energy consumption of trains. For this reason, the optimization of the passenger demand satisfaction and energy consumption requires research in both the line planning and the train diagram aspects.

Motivated by these, this paper aims to solve a multi-cycle train timetable scheduling problem by a space-time network with the joint optimization of the supply-to-demand relationship and energy consumption. To this end, we need to solve the following issues: (1) How to harmonize the relationship between line planning and timetabling to meet the time-varying passenger demand. (2) How to establish a comprehensive optimization model for scheduling a multi-cycle timetable. The model should have the ability to describe the difference in energy consumption caused by combinations of stopping and crossing in stations while focusing on the degree of passenger demand satisfaction, and then optimize both. (3) How to improve the efficiency of the model solution by a suitable algorithm in the face of complex cases.

1.2. Literature Reviews

The concept of a periodic train timetable was first proposed in the Netherlands in 1931, and the cycle time was set to 1 h. A cyclic timetable has many advantages, such as a strong regularity, flexible use, high-capacity utilization rate and convenient travel for passengers [1]. In 1989, Serafini and Ukovich [2] proposed the periodic event scheduling problem (PESP). Later, many scholars studied the cyclic train timetable problem based on the PESP model framework [3–7]. Mathias [8] introduced the time-discrete technology into the PESP model and proposed the integer programming formula. In addition to the PESP model, some scholars also used time–space networks to solve the cyclic train timetable problem. Caprara et al. [9] proposed a graph theoretic formulation for the periodic train timetable problem. On this basis, Zhang et al. [10] introduced the construction of an extended spatial-temporal network and proposed a new type of integer programming model reformulation for the cyclic train timetabling problem on a double-track railway corridor.

Some studies tried to take different approaches to meet the demand for peak and off-peak hours. Wang Bo et al. [1] used the method of cancelling train lines to meet the different passenger flow demands during peak and off-peak periods. However, the cancellation of train lines would destroy the regularity of train services. In addition, other studies used a multi-cycle train timetable to improve the meeting of demand. Odijk [11] proposed the concept of a multi-cycle train timetable. Robenek et al. [12] designed a multi-cycle timetable optimization model with the goal of maximizing passenger satisfaction. Zhou [13] constructed an optimization model for solving a multi-cycle train timetable problem with a fixed cycle length and solved the model by using the Lagrangian relaxation algorithm. Zhou [14] was devoted to modeling the multi-periodic train timetable problem, which collaboratively optimized the operation periods, arrival times and departure times of all period types of trains. Yan [15] proposed a multi-frequency line planning problem and multi-period train timetable problem model, with consideration of both the periodic and

aperiodic nature to meet strongly heterogeneous train services and reduce the capacity loss of train operating companies.

In terms of the objective of timetable optimization, Niu et al. [16] proposed a set of quadratic and quasi-quadratic objective functions to accurately formulate the total waiting time under the minute-related demand and hour-related demand of different origin–destination (OD) pairs so that the total station passenger waiting time is the smallest, and a general advanced solver is used to solve the model. The cyclic train timetable problem usually considers passenger-related expenses as the objective function, such as a minimum train waiting time [17], guaranteed maximum passenger transfer waiting time, reduction in the maximum train dwell time [18] and maximum passenger demand satisfaction [19]. Yin [20] minimized the weighted value of the total train travel time and the total passenger waiting time, considering vehicle turnover as the objective function.

The existing studies have shown that factors such as the running time, headway time and stop pattern affect the energy consumption of the train [21,22]. Some research was mainly focused on the calculation of the energy consumption, train running control by analytical models [23], optimization models [24–28] and simulation-based approaches [29–31]. Some studies tried to schedule train diagrams with considerations of railway energy consumption. Dingjun Chen [32] established an energy-efficient operation diagram for high-speed railways based on stop and dispatch optimization. Huiru Zhang [33] developed a two-layer planning model for the timetable optimization of a high-speed rail based on energy-efficient train control. Albrecht [34] developed a new approach to integration for balancing simultaneity and energy efficiency in train schedules. Li [35] established a multi-objective train scheduling model and integrated goals for energy efficiency, emissions reduction and travel time. Lancien [36] minimized the energy consumption of trains under fixed service time conditions by data mining and an optimization model. Bai Yun [37] studied the energy consumption at different inertial distances before braking and at lower speed limits, as well as the uniformity of train speed by train motion analysis and simulation.

Despite the fruitful results of the current research, there are still some aspects that need to be studied: (1) the existing multi-cycle timetabling models generally take the line planning as determined input and have not yet integrated the cycle and train-specific space–time points for optimization; (2) the existing multi-cycle models generally model by the station entry and exit throats, which cannot distinguish the difference in the energy consumption of trains under different stopping modes; and (3) the existing algorithms cannot balance the efficiency and accuracy of the algorithm for the above-mentioned model.

1.3. Potential Contributions

In order to solve the issues mentioned in Section 1.1 and jointly optimize the supply-to-demand relationship and energy consumption, the line plan and timetable would be optimized simultaneously. The line plan, which is composed of lines, is one of the most basic elements for rail transit operations. A line represents a series of trains that have the same route, stopping pattern, frequency and cycle length, where the route is in a high-level infrastructure graph, ignoring the precise details of the platforms, junctions, etc. [38]. The train timetable determines the arrival and departure time of trains at stations based on the line plan. In the multi-cycle train timetable, trains belonging to different train lines have an identical cycle length, with a designed route and stop plan [38].

This paper uses a spatial-temporal network for modeling and designs the objective function and solution framework. A multi-cycle timetable considering the supply-to-demand relationship and energy consumption (MTSDE) is proposed to solve such an issue. The potential contributions are as follows:

1. A periodized spatial-temporal network that can support the integrated optimization of passenger service satisfaction and energy consumption is studied. To describe the acceleration and deceleration behavior of trains due to stopping, a vertex set and an arc set of the spatial-temporal network are created based on the decomposed actions of the trains' movements. The network can be used to determine the spatial-temporal path of trains, which in turn enables the integrated optimization of passenger service satisfaction and energy consumption.
2. An integrated optimization model taking the train spatial-temporal path, cycle length and active lines as the variables is proposed. The objective function composes the supply–demand matching degree (SDMD), the minimum time cost (MTC) and the energy consumption (EC), where the SDMD is measured by the difference between the demand flow and train frequency in each time duration, and the MTC and EC are measured by the costs of the spatial-temporal paths. Four classes of constraints are considered, including the train flow balance constraints, cycle interval constraints, incompatible constraints and minimum travel time constraints.
3. A hybrid heuristic Lagrangian decomposition method is proposed. The determination of the cycle length and line and the scheduling of the spatial-temporal points in the train diagram are separated, where the scheduling of the train diagram is further decomposed into an independent problem by the Lagrangian relaxation.

The rest of this paper is organized as follows: In Section 2, the model of the MTSDE is introduced with the objective function and constraint conditions based on periodized spatial-temporal networks. Then, for solving the complex model, a hybrid heuristic Lagrangian decomposition method is proposed. In Section 3, cases under different passenger flow demand scenarios are performed to analyze the characteristics of the MTSDE by comparisons with a single-cycle train timetable. Moreover, the solving performance of the proposed model is compared with the commercial solver. Lastly, the real-world case is analyzed to verify the applicability of the MTSDE.

2. Methodology

The MTSDE contains three parts: The periodized spatial-temporal network, the optimization model and the decomposition algorithm. The periodized spatial-temporal network focuses on how to build vertex and arc sets to describe the differential operation of trains, which in turn supports the subsequent model construction. The optimization model considers elements of timetabling and line planning, where elements of line planning determine the path, cycle length and stopping patterns, and the elements of timetabling determine the specific spatial-temporal points of trains. In addition, the model's objective function is composed of supply demand matching degree (SDMD), the minimum time cost (MTC) and the energy consumption (EC); the model is constrained by train flow balance constraints, cycle interval constraints, incompatible constraints and minimum travel time constraints. Based on characteristics of the spatial-temporal network and the model, the decomposition algorithm optimizes the line planning elements and timetable elements in stages and achieves efficient preparation of multi-cycle complex operation diagrams by Lagrangian relaxation algorithm.

The assumptions of the model are as follows:

1. The supply–demand matching set in this paper focuses on the supply–demand matching of several stations. We believe that the trains' transportation capacity in a line needs to be prioritized to satisfy the stations with larger passenger flows, and other stations with smaller passenger flows can be appropriately ignored. Therefore, the set of stations to be concerned and their corresponding passenger flows will be given in the modeling process of this paper. This assumption is in line with the planning convention in actual transportation organization.

2. The numbers of passengers on board in each station are preset as an input for the model. In the course of practical application, the specific OD volume and dynamic upload and download of passenger flow is difficult to count. We pre-estimate the numbers of passenger that can be served in each station by means of passenger ticket allocation techniques.
3. The time resolution of the spatial-temporal network is set to 1 min.

We introduce the notations and modeling basics first.

2.1. Notations and Modeling Basis

For the convenience of description, the sets, parameters and decision variables notations involved in this paper are shown in Table 1.

Table 1. Notaions.

Type	Notation	Definition
Set	K	Set of trains $k \in K$
	Π	Set of line plan $\Pi = \{1, 2, \ldots, \pi, \ldots, n\}$, where π is the element of line plan
	o_π	Origin station index of line π
	d_π	Destination station index of line π
	S	Set of stations
	S_π	Set of stations along line π's route
	$\overline{S}_\pi$	Set of no-skip stations along line π's route
	K_π	Set of trains belonging to a line π, where $K_\pi \subset K$, $\pi \in \Pi$
	M	The number of time durations used for calculating passenger demand satisfaction. $M = \{1, 2, \ldots, m, \ldots, n_t\}$, where n_t is the number of time duration. These time durations are divided from the whole-time horizon T.
	S_o	Stations, whose degree of passenger satisfaction needs to be optimized. Generally speaking, it is the stations in the line with high passenger flow.
Parameter	g_i	Minimum arrival headway of station $s_i \in S$
	h_i	Minimum departure headway of station $s_i \in S$
	m_i	Number of side tracks in station $s_i \in S$. If the station has overtravel conditions $m_i \geq 1$, $m_i = 0$ otherwise.
	m_i'	Number of main tracks in station $s_i \in S$
	c_k'	The unit cost for train k stopping in a station
	p_k	The earliest allowed start time of train k for running
	q_k	The latest allowed end time of train k for running
	α_{ki}	The pure running time for train k to traverse section $s_i - s_{i+1}$
	α_k'	Additional time for train k caused by acceleration
	α_k	Additional time for train k caused by deceleration
	β_{ki}	The minimum required dwell time of train k at station s_i
	c_k	Operating cost unit time for train k to run
	f_π	The departure frequency of the line π in the time range T
	w_π	Index of the first train in a line π
	q_π^k	The order of train k in line π
	τ_π	The time interval between two consecutive trains in the same line π
	σ_i^π	Numbers of passengers that can be served in station i by a train in line planning π. If $i \in \overline{S}_\pi$, then $\sigma_i^k = 0$, else $\sigma_i^k = \mathbb{N}$.
	δ_t^i	Passenger demand at station i at time t
	ts_m	Start time of the mth time duration, $ts_m = \Delta(m-1)$
	te_m	The end time of the mth time duration, $te_m = \Delta m - 1$
	$\theta_t^{k,s}$	Coefficient of dwelling or waiting energy consumption per time of train k
	$\theta_t^{k,r,da}$	Coefficient of running energy consumption per time of train k's departure–arrival arcs
	$\theta_t^{k,r,dp}$	Coefficient of running energy consumption per time of train k's departure–passing arcs
	$\theta_t^{k,r,pa}$	Coefficient of running energy consumption per time of train k's passing–arrival arcs
	$\theta_t^{k,r,pp}$	Coefficient of running energy consumption per time of train k's passing–passing arcs
	$\xi_t^k(u,v)$	Time cost of arcs $u \to v$ of train k
	$\xi_e^k(u,v)$	Energy cost of arcs $u \to v$ of train k
Variable	$x_{uv}^{k,\pi}$	If the train k of line π is passing through arc $u \to v$, then $x_{uv}^{k,\pi} = 1$, else $x_{uv}^{k,\pi} = 0$
	pl_π	Cycle length of line π
	y_π	If line π is chosen, then $y_\pi = 1$, else $y_\pi = 0$

In multi-cycle train timetable, trains belonging to different lines have different cycle length, and trains belonging to the same line have the same cycle length and the stop pattern. The arrival and departure time of trains in sections and stations strictly meet the feasibility of capacity utilization. Figure 1 is a sample of multi-cycle train timetable.

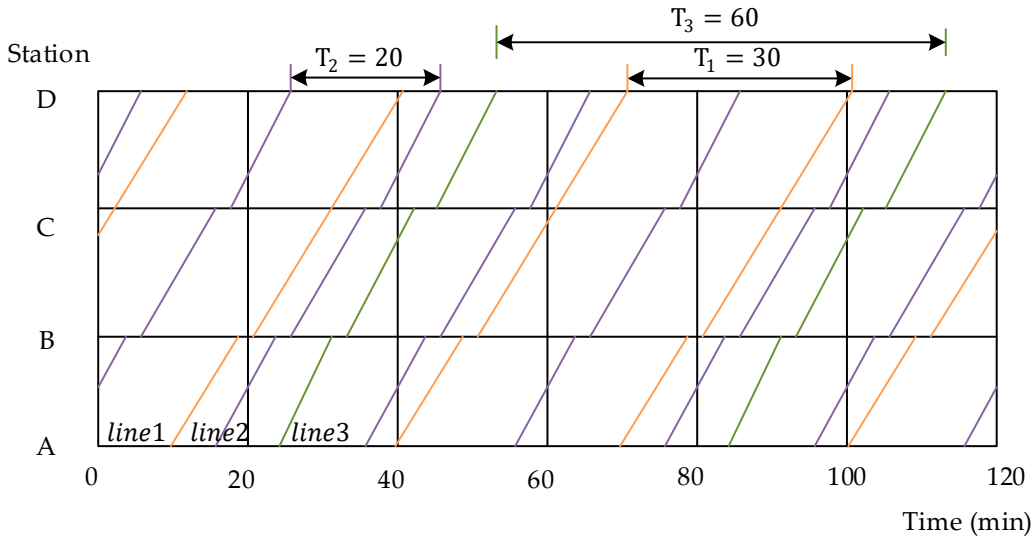

Figure 1. A multi-cycle train timetable with three-cycle period. There are 3 train lines. The cycle length of line 1 is 30 min, and the train belonging to line 1 departs every 30 min. The cycle length of line 2 is 20 min, and the train belonging to line 2 departs every 20 min. The cycle length of line 3 is 60 min, and trains belonging to line 3 depart every 60 min.

The difficulty of multi-cycle train timetable problem is how to determine the cycle length and departure time so that the multi-cycle train timetable can meet the demands of passengers in different time durations and also minimizing the energy cost.

2.2. Augmented Spatial-Temporal Network for Multi-Cycle Timetabiling

The augmented spatial-temporal network can extend spatial-temporal vertexes according to cycles. Thus, trains belonging to a certain line will have a unique spatial-temporal network after determining a cycle length. The vertexes and arcs of this network have certain characteristics.

2.2.1. Spatial-Temporal Vertexes for Augmented Spatial-Temporal Network

For any train $k \in K$, the outflows and inflows at both the origin point $\overline{o}$ and the destination point $\overline{d}$ are both set as 1. Assume that the train can only stop on the side track of the station, and the main track can only be used for passing. Thus, the main track of a station is regarded as a node $\varphi_{t,i}^{k,\pi}$ in spatial-temporal network. Generally speaking, a station is configured with only one main track in one direction. Moreover, consider the side tracks as two nodes $\rho_{t,i,l}^{k,\pi}$ and $\overline{\rho}_{t,i,l}^{k,\pi}$, respectively. In order to express the movement of trains between stations, $\sigma_{t,i}^{k,\pi}$ nodes are introduced to describe the running behavior of trains between stations. Therefore, suppose that the station s_i has $m_i \in N$ side tracks and $m_i' \in \{0,1\}$ main tracks and consider that the nodes will repeat $\left[\frac{T}{pl_\pi}\right]$ times in the whole time horizon T; then, there are $2+\sum_{i=1}^{n}(2m_i+m_i'+1)\cdot\left[\frac{T}{pl_\pi}\right]$ nodes in the spatial-temporal network G_k of train k. The node set is shown as Equation (1):

$$V^k = \left\{\overline{o},\overline{d}\right\} \cup \left[\left\{\left(\rho_{t,i,l}^{k,\pi},\overline{\rho}_{t,i,l}^{k,\pi}\right)\right\} \cup \left\{\varphi_{t,i}^{k,\pi}\right\} \cup \left\{\sigma_{t,i}^{k,\pi}\right\}\right]_{t\in[0,\cdot pl_\pi\cdot q_\pi^k]} \quad i=1,2,\cdots,n; l=1,2,\cdots m_i; pl_\pi=1,\cdots,\left[\frac{T}{pl_\pi}\right] \tag{1}$$

2.2.2. Arc Set Considering Differences in Energy Consumption for Various Train Behaviors

In the train spatial-temporal network, the spatial-temporal arc set A^k contains nine kinds of spatial-temporal arcs, as shown in Table 2. The train starting arc represents that at time $t \geq p_k$, train k starts its running operation from station s_{o_π}. The train ending arc represents that at time $t \leq q_k$, train k completes its running operation at station s_{d_π}. The train dwelling arc refers to the process of minimum dwell time for train k to stop at the lth platform track of station s_i, during period $[t, t']$. If the train has additional stop time, it needs to enter the train waiting arc; train waiting arc refers to the process which a train continues to stay on the lth platform track at station s_i during $[t, t']$, after meeting its minimum dwell time requirements. In order to express the process of the train leaving the station from the platform, the train departure arc is introduced. Train departure arc refers to the train starts from the platform l of the s_i station where the stopped trains leave the station at the time point t. In order to illustrate trains running processes in the section from s_i to next station s_{i+1}, and depict different operation modes in the section, including departure–arrival, departure–passing, passing–arrival and passing–passing, we design four corresponding train arcs, respectively. Train departure–arrival arc refers to a running process that the train stops at s_i station and stops at the lth platform of the station s_{i+1} in period $[t, t']$. Likewise, train departure–passing arc refers to a running process that the train stops at s_i station and skips the s_{i+1} station in period $[t, t']$. Train passing–arrival arc represents a running process that the train skips s_i station and stops at the lth platform of the station s_{i+1} in period $[t, t']$. Train passing–passing arc represents a running process that the train skips s_i station and skips the s_{i+1} station in period $[t, t']$. All the train arcs have time cost ξ_t^k and some of them have energy cost ξ_e^k.

Table 2. The arc set of spatial-temporal network.

ID	Name	Notation	Time Cost and Energy Cost of Arcs	Set
1	Train starting arcs	$\overline{o} \to \rho_{t,i,l}^{k,\pi}$	For $\pi \in \Pi, k \in K_\pi$, if $i = s_{o_\pi}$ and $t \geq p_k$, then the time cost of arc $\overline{o} \to \rho_{t,i,l}^{k,\pi}$ is $\xi_t^k\left(\overline{o} \to \rho_{t,i,l}^{k,\pi}\right) = 0$; else $\xi_t^k\left(\overline{o} \to \rho_{t,i,l}^{k,\pi}\right) = +\infty$. where $i \in \{1, 2, \cdots, n-1\}$; $l \in \{1, 2, \cdots m_i\}$; $t \in \{0, 1, \cdots, T\}$	$A_s^{k,\pi}$
2	Train ending arcs	$\sigma_{t,i}^{k,\pi} \to \overline{d}$	For $\pi \in \Pi, k \in K_\pi$, if $i = s_{d_\pi}$ and $t \leq q_k$, then the time cost of arc $\sigma_{t,i}^{k,\pi} \to \overline{d}$ is $\xi_t^k\left(\sigma_{t,i}^{k,\pi} \to \overline{d}\right) = 0$; else $\xi_t^k\left(\sigma_{t,i}^{k,\pi} \to \overline{d}\right) = +\infty$. where $i \in \{2, 3, \cdots, n\}$; $t \in \{0, 1, \cdots, T\}$	$A_e^{k,\pi}$
3	Train dwelling arcs	$\rho_{t,i,l}^{k,\pi} \to \overline{\rho}_{t',i,l}^{k,\pi}$	For $\pi \in \Pi, k \in K_\pi$, if $s_{o_\pi} \leq i \leq s_{d_\pi}$ and $s_i \in S \backslash \overline{S}_k$, then the time cost of arc $\rho_{t,i,l}^{k,\pi} \to \overline{\rho}_{t',i,l}^{k,\pi}$ is $\xi_t^k\left(\rho_{t,i,l}^{k,\pi} \to \overline{\rho}_{t',i,l}^{k,\pi}\right) = c_k^{'}(t'-t)$, else $\xi_t^k\left(\rho_{t,i,l}^{k,\pi} \to \overline{\rho}_{t',i,l}^{k,\pi}\right) = +\infty$. In addition, the energy cost of this arc is $\xi_e^k\left(\rho_{t,i,l}^{k,\pi} \to \overline{\rho}_{t',i,l}^{k,\pi}\right) = \xi_t^k\left(\rho_{t,i,l}^{k,\pi} \to \overline{\rho}_{t',i,l}^{k,\pi}\right) \cdot \theta_t^{k,s}$. $\theta_t^{k,s}$ is the coefficient of dwelling or waiting energy consumption per time of train k. where $i \in \{1, 2, \cdots, n\}$, $l \in \{1, 2, \cdots m_i\}$, $t, t' \in \{0, 1, \cdots, T\}$.	$A_{ds}^{k,\pi}$
4	Train waiting arcs	$\overline{\rho}_{t,i,l}^{k,\pi} \to \overline{\rho}_{t+1,i,l}^{k,\pi}$	For $\pi \in \Pi, k \in K_\pi$, if $s_{o_\pi} \leq i \leq s_{d_\pi}$ and $s_i \in S \backslash \overline{S}_k$, $p_k \leq t \leq q_k - 1$, then the time cost of arc $\overline{\rho}_{t,i,l}^{k,\pi} \to \overline{\rho}_{t+1,i,l}^{k,\pi}$ is $\xi_t^k\left(\overline{\rho}_{t,i,l}^{k,\pi} \to \overline{\rho}_{t+1,i,l}^{k,\pi}\right) = c_k^{'}$, else $\xi_t^k\left(\overline{\rho}_{t,i,l}^{k,\pi} \to \overline{\rho}_{t+1,i,l}^{k,\pi}\right) = +\infty$. In addition, the energy cost of this arc is $\xi_e^k\left(\overline{\rho}_{t,i,l}^{k,\pi} \to \overline{\rho}_{t+1,i,l}^{k,\pi}\right) = \xi_t^k\left(\overline{\rho}_{t,i,l}^{k,\pi} \to \overline{\rho}_{t+1,i,l}^{k,\pi}\right) \cdot \theta_t^{k,s}$. where $i \in \{1, 2, \cdots, n\}$, $l \in \{1, 2, \cdots m_i\}$, $t \in \{0, 1, \cdots, T-1\}$	
5	Train departure arcs	$\overline{\rho}_{t,i,l}^{k,\pi} \to \sigma_{t,i}^{k,\pi}$	For $\pi \in \Pi, k \in K_\pi$, if $s_{o_\pi} \leq i \leq s_{d_\pi}$ and $s_i \in S \backslash \overline{S}_k$, $t \leq q_k$, then the time cost of arc $\overline{\rho}_{t,i,l}^{k,\pi} \to \sigma_{t,i}^{k,\pi}$ is $\xi_t^k\left(\overline{\rho}_{t,i,l}^{k,\pi} \to \sigma_{t,i}^{k,\pi}\right) = 0$, else $\xi_t^k\left(\overline{\rho}_{t,i,l}^{k,\pi} \to \sigma_{t,i}^{k,\pi}\right) = +\infty$. The set of $\overline{\rho}_{t,i,l}^{k,\pi} \to \sigma_{t,i}^{k,\pi}$ is denoted by A_{dep}^k. where $i \in \{1, 2, \cdots, n\}$, $l \in \{1, 2, \cdots m_i\}$, $t, t' \in \{0, 1, \cdots, T\}$	$A_{de}^{k,\pi}$

Table 2. *Cont.*

ID	Name	Notation	Time Cost and Energy Cost of Arcs	Set
6	Train departure–arrival arcs in section	$\sigma_{t,i}^{k,\pi} \to \rho_{t',i+1,l}^{k,\pi}$	For $\pi \in \Pi, k \in K_\pi$, if $s_{o_\pi} \le i \le s_{d_\pi} - 1$ and $s_i \in S \backslash \overline{S}_k$, $s_{i+1} \in S \backslash \overline{S}_k$, $t \ge p_k$, and $t' = t + \alpha_{\mathrm{ki}} + \alpha_k^{'} + \alpha_k^{''} \le q_k$, then the time cost of arc $\sigma_{t,i}^{k,\pi} \to \rho_{t',i,l}^{k,\pi}$ is $\xi_t^k\left(\sigma_{t,i}^{k,\pi} \to \rho_{t',i,l}^{k,\pi}\right) = c_k(t'-t)$, else $\xi_t^k\left(\sigma_{t,i}^{k,\pi} \to \rho_{t',i,l}^{k,\pi}\right) = +\infty$. In addition, the energy cost of this arc is $\xi_e^k\left(\sigma_{t,i}^{k,\pi} \to \rho_{t',i,l}^{k,\pi}\right) = \xi_t^k\left(\sigma_{t,i}^{k,\pi} \to \rho_{t',i,l}^{k,\pi}\right) \cdot \theta_t^{k,r,da}$. $\theta_t^{k,r,da}$ is the coefficient of running energy consumption per time of train k. where $i \in \{1,2,\cdots,n-1\}$, $l \in \{1,2,\cdots m_{i+1}\}$, $t,t' \in \{0,1,\cdots,T\}$	$A_{trv}^{k,\pi}$
7	Train departure–passing arcs in section	$\sigma_{t,i}^{k,\pi} \to \varphi_{t',i+1}^{k,\pi}$	For $\pi \in \Pi, k \in K_\pi$, if $s_{o_\pi} \le i \le s_{d_\pi} - 1$ and $s_i \in S \backslash \overline{S}_k$, $s_{i+1} \in S_k$, $t \ge p_k$, $t' = t + \alpha_{ki} + \alpha_k^{'} \le q_k$, then the time cos t of arc $\sigma_{t,i}^{k,\pi} \to \varphi_{t',i+1}^{k,\pi}$ is $\xi_t^k\left(\sigma_{t,i}^{k,\pi} \to \varphi_{t',i+1,l}^{k,\pi}\right) = c_k(t'-t)$, else $\xi_t^k\left(\sigma_{t,i}^{k,\pi} \to \varphi_{t',i+1,l}^{k,\pi}\right) = +\infty$. In addition, the energy cost of this arc is $\xi_e^k\left(\sigma_{t,i}^{k,\pi} \to \varphi_{t',i+1,l}^{k,\pi}\right) = \xi_t^k\left(\sigma_{t,i}^{k,\pi} \to \varphi_{t',i+1,l}^{k,\pi}\right) \cdot \theta_t^{k,r,dp}$. where $i \in \{1,2,\cdots,n-1\}$, $t,t' \in \{0,1,\cdots,T\}$	
8	Train passing–arrival arcs in section	$\varphi_{t,i}^{k,\pi} \to \rho_{t',i+1,l}^{k,\pi}$	For $\pi \in \Pi, k \in K_\pi$, if $s_{o_\pi} \le i \le s_{d_\pi} - 1$ and $s_i \in S_k$, $s_{i+1} \in S \backslash \overline{S}_k$, $t \ge p_k$, $t' = t + \alpha_{ki} + \alpha_k^{''} \le q_k$, then the time cost of arc $\varphi_{t,i}^{k,\pi} \to \rho_{t',i+1,l}^{k,\pi}$ is $\xi_t^k\left(\varphi_{t,i}^{k,\pi} \to \rho_{t',i+1,l}^{k,\pi}\right) = c_k(t'-t)$, else $\xi_t^k\left(\varphi_{t,i}^{k,\pi} \to \rho_{t',i+1,l}^{k,\pi}\right) = +\infty$. In addition, the energy cost of this arc is $\xi_e^k\left(\varphi_{t,i}^{k,\pi} \to \rho_{t',i+1,l}^{k,\pi}\right) = \xi_t^k\left(\varphi_{t,i}^{k,\pi} \to \rho_{t',i+1,l}^{k,\pi}\right) \cdot \theta_t^{k,r,pa}$. where $i \in \{1,2,\cdots,n-1\}$, $l \in \{1,2,\cdots m_{i+1}\}$, $t,t' \in \{0,1,\cdots,T\}$	
9	Train passing–passing arcs in section	$\varphi_{t,i}^{k,\pi} \to \varphi_{t',i+1}^{k,\pi}$	For $\pi \in \Pi, k \in K_\pi$, if $s_{o_\pi} \le i \le s_{d_\pi} - 1$ and $s_i \in S_k$, $s_{i+1} \in S_k$, $t \ge p_k$, $t' = t + \alpha_{ki} \le q_k$, then the time cost of arc $\varphi_{t,i}^{k,\pi} \to \varphi_{t',i+1}^{k,\pi}$ is $\xi_t^k\left(\varphi_{t,i}^{k,\pi} \to \varphi_{t',i+1}^{k,\pi}\right) = c_k(t'-t)$, else $\xi_t^k\left(\varphi_{t,i}^{k,\pi} \to \varphi_{t',i+1}^{k,\pi}\right) = +\infty$. In addition, the energy cost of this arc is $\xi_e^k\left(\varphi_{t,i}^{k,\pi} \to \varphi_{t',i+1}^{k,\pi}\right) = \xi_t^k\left(\varphi_{t,i}^{k,\pi} \to \varphi_{t',i+1}^{k,\pi}\right) \cdot \theta_t^{k,r,pp}$ where $i \in \{1,2,\cdots,n-1\}$, $t,t' \in \{0,1,\cdots,T\}$	
				A

2.3. Optimization Model for Scheduling MTSDE

The core of the proposed model is to find the shortest paths of trains under the time and energy costs and find the best combination of such paths based on spatial-temporal network. On the basis of spatial-temporal network, the establishment original model P of MTSDE is established, as shown in Equations (2)–(9).

2.3.1. Objective Function

The objective function of MTSDE includes the total time cost of all trains, the total energy cost and the sum of the differences between the station passenger demand and the train supply. According to the design of spatial-temporal network, the objective function is shown as Equation (2). Elements in Equations (2)–(11) are shown in Table 1.

$$Min \sum_{k \in K} \sum_{u \to v \in A^k} \left(\xi_t^k(u,v) + \rho_1 \xi_e^k(u,v)\right) \cdot x_{uv}^{k,\pi} + \rho_2 \sum_{i \in S_o} \sum_{m \in M} \left| \sum\nolimits_{t \in [ts_m, te_m]} \delta_t^i - \sum\nolimits_{t \in [ts_m, te_m]} \sum_{\pi \in \Pi} y_\pi \cdot \frac{T}{pl_\pi \cdot m} \cdot \sigma_i^\pi \right| \quad (2)$$

where $\left(\xi_t^k(u,v) + \rho_1 \xi_e^k(u,v)\right) \cdot x_{uv}^{k,\pi}$ is the cost of time and energy cost in arc $u \to v$ of train k and line π. ρ_1 and ρ_2 are two coefficients for weighting importance of different parts in Equation (2).

In order to describe the relationship between passenger demand and train supply more accurately, it is necessary to divide the time of day into multiple time periods and match the passenger demand and train supply in each time period, so as to achieve the matching of supply and demand throughout the whole-time horizon. Thus, in Equation (2), $y_\pi \cdot \frac{T}{pl_\pi \cdot m} \cdot \sigma_i^\pi$ represents the average number of service passengers at time t by line π. Then, $\sum_{t\in[ts_m,te_m]} \delta_t^i - \sum_{t\in[ts_m,te_m]} \sum_{\pi\in\Pi} y_\pi \cdot \frac{T}{pl_\pi \cdot m} \cdot \sigma_i^\pi$ calculates the difference in passenger demand in station i and the train supply in time duration m.

2.3.2. Constraint Condition

The constraints of MTSDE consist of four classes: train flow balance constraints, cycle interval constraints, incompatible constraints and minimum travel time constraints.

(a) Train flow balance constraints

Equation (3) indicates that the train can only belong to one line π with origin point $\overline{o}$. The line determines the cycle length and stopping plan directly. Because there are no arcs between layers with different cycles, the train cycle will be fixed in a path. Equations (3)–(5) are the train flow balance constraints.

$$\sum_{\pi\in\Pi} \sum_{\{v:\widetilde{o}\to v\in A^k\}} x_{\widetilde{o}v}^{k,\pi} = 1, \forall k \in K \tag{3}$$

$$\sum_{\pi\in\Pi} \sum_{\{u:u\to\widetilde{d}\in A^k\}} x_{u\widetilde{d}}^{k,\pi} = 1, \forall k \in K \tag{4}$$

$$\sum_{\{u:u\to v\in A^k\}} x_{uv}^{k,\pi} = \sum_{\{w:v\to w\in A^k\}} x_{vw}^{k,\pi}, \forall \pi \in \Pi, \forall k \in K_\pi; v \in V^k \backslash \left\{\overline{O}, \overline{d}\right\} \tag{5}$$

(b) Cycle interval constraints

In order to ensure the time relation between the first train and other trains can satisfy the cycle requirement, Equation (7) ensures that, for any line π with cycle length pl_π, arcs of each train k in π are all coupled with the first train w_π in line π, i.e., the time interval between each train and the first train is a multiple of the cycle and train order—1 $\widetilde{t} = t + \left(q_\pi^k - 1\right) \cdot pl_\pi$. We define a function $FT(\cdot, t)$ that can find the elements from arc subset $sA \in A$, where the elements' time is t.

$$\begin{aligned} x_{u,v:\ (u,v)\in FT(sA,t)}^{w_\pi,\pi} &= x_{u,v:\ (u,v)\in FT(sA,\widetilde{t})}^{k,\pi} \\ sA \in A = \left\{A_s^{k,\pi}, A_e^{k,\pi}, A_{ds}^{k,\pi}, A_{de}^{k,\pi}, A_{trv}^{k,\pi}\right\},\ &\forall \pi \in \Pi, k \in K_\pi, \widetilde{t} = t + \left(q_\pi^k - 1\right) \cdot pl_\pi,\ \forall t, \widetilde{t} \in T, q_\pi^k > 1 \end{aligned} \tag{6}$$

(c) Incompatible constraint

Equation (8) is an incompatible constraint to prevent unsafe following behaviors of trains in sections and stations. Where $\mathcal{C}$ is an incompatible set, and its detailed setting can be seen in Section 2.3.3,

$$\sum_{\pi\in\Pi} \sum_{k\in K} \sum_{u\to v\in c} x_{uv}^{k,\pi} \le 1, \forall c \in \mathcal{C} \tag{7}$$

(d) Minimum travel time constraint

Equation (9) is the minimum travel time constraint, which focuses on the travel time of train k cannot be higher than the time threshold η.

$$\sum_{v\in V_k} a_{kv} + a_k' \left(\sum_{u\to v\in A^k} x_{uv}^{k,\pi} - 1 \right) + a_k'' \left(\sum_{u\to v\in A^k} x_{uv}^{k,\pi} - 1 \right) \le \eta, \forall \pi \in \Pi, k \in K_\pi \tag{8}$$

(e) Decision variables

Equation (10) specifies the types of decision-making variables.

$$x_{uv}^{k,\pi} \in \{0,1\}, \forall \pi \in \Pi, k \in K_\pi; u \to v \in A^k \tag{9}$$

$$y_\pi \in \{0,1\}, \forall \pi \in \Pi \tag{10}$$

$$pl_\pi \in \mathbb{N}, \forall \pi \in \Pi \tag{11}$$

2.3.3. Sets of Incompatible Arcs

There are some conditions that must be met in the actual operation, such as train following headway constraints, no overtaking constraints, etc. In the spatial-temporal network, these conditions are represented by the sets of incompatible arcs $\mathcal{C}$ (which is important in Equation (7)). $\mathcal{C}$ represents that, in a specified space and time, at most one arc can be chosen from the arc sets. $\mathcal{C}$ includes five subsets: arrival headway constraint arc set, departure headway constraint arc set, interval forbidden crossing constraint arc set, platform track exclusive constraint arc set. These are

$$\begin{array}{l}\mathcal{C} = \left\{C^1_{it} \middle| i = 2,3,\ldots,n; t = 0,1,\ldots,T - g_i + 1\right\} \\ \left\{C^2_{it} \middle| i = 1,2,\ldots,n-1; t = 0,1,\ldots,T - h_i + 1\right\} \\ \left\{C^{2\prime}_{it} \middle| i = 1,2,\ldots,n-1; t = 0,1,\ldots,T - \rho + 1\right\} \\ \left\{C^3_{it_1t_2} \middle| i = 1,2,\ldots,n-1; 0 \le t_1 < t_2 < T \; s.t. B_{it_1t_2}, B'_{it_1t_2} \ne \varnothing\right\} \\ \left\{C^4_{ilt} \middle| i = 1,2,\ldots,n; l = 1,2,\ldots,m_i; t = 0,1,\ldots,T\right\} \\ \left\{C^5_{it_1t_2} \middle| i = 1,2,\ldots,n-1; 0 \le t_1 < t_2 < T\right\}\end{array} \tag{12}$$

(a) Incompatible arcs for arrival headway constraint

For any station i, the arrival between adjacent trains is constrained by the minimum arrival interval g_i. Let t be the time when the train leaves from station s_{i-1} (including the departure after stopping and passing through without stopping), and t' be the time when the train arrives at station i (including stopping and passing through). Then, for any time t_1 at station i, there is a set of incompatible constraints $C^1_{it_1}$ in the closed interval of $t' \in [t_1, t_1 + g_i - 1]$. The set includes four types of spatial-temporal arcs, namely train departure–arrival arcs in section $\sigma^{k,\pi}_{t,i-1} \to \rho^{k,\pi}_{t',i,l}$, train departure–passing arcs in section $\varphi^{k,\pi}_{t,i-1} \to \rho^{k,\pi}_{t',i,l}$, train passing–arrival arcs in section $\sigma^{k,\pi}_{t,i-1} \to \varphi^{k,\pi}_{t',i}$ and train passing–passing arcs in section $\varphi^{k,\pi}_{t,i-1} \to \varphi^{k,\pi}_{t',i}$. When one of these arcs is selected ($x^{k,\pi}_{uv} = 1$), the other arcs cannot be selected.

$$\begin{array}{l}C^1_{it_1} = A \cap [\left\{\sigma^{k,\pi}_{t,i-1} \to \rho^{k,\pi}_{t',i,l} \middle| l = 1,2,\ldots m_i; t,t' = 0,1,\ldots,T; t_1 \le t' \le t_1 + g_i - 1\right\} \\ \quad \cup \left\{\varphi^{k,\pi}_{t,i-1} \to \rho^{k,\pi}_{t',i,l} \middle| m'_{i-1} = 1; l = 1,2,\ldots m_i; t,t' = 0,1,\ldots,T; t_1 \le t' \le t_1 + g_i - 1\right\} \\ \quad \cup \left\{\sigma^{k,\pi}_{t,i-1} \to \varphi^{k,\pi}_{t',i} \middle| m'_i = 1; t,t' = 0,1,\ldots,T; t_1 \le t' \le t_1 + g_i - 1\right\} \\ \quad \cup \left\{\varphi^{k,\pi}_{t,i-1} \to \varphi^{k,\pi}_{t',i} \middle| m'_{i-1} = m'_i = 1; t,t' = 0,1,\ldots,T; t_1 \le t' \le t_1 + g_i - 1\right\} t,]\end{array} \tag{13}$$

(b) Departure headway constraint

For any station i, the departure of its trains is constrained by the minimum departure interval h_i. Let t be the time when the train leaves from station s_i (including stop and leave and pass without stop), and t' be the time when the train arrives at station s_{i+1} (including stopping and passing). Then, for any time t_1 at station i, there is a set of incompatible constraints $C^2_{it_1}$ in the closed interval of $t' \in [t_1, t_1 + h_i - 1]$. The set includes four types of spatial-temporal arcs, respectively, train departure–arrival arcs $\sigma^{k,\pi}_{t,i} \to \rho^{k,\pi}_{t',i+1,l}$, train departure–passing arcs $\varphi^{k,\pi}_{t,i} \to \rho^{k,\pi}_{t',i+1,l}$, train passing–arrival arcs $\sigma^{k,\pi}_{t,i} \to \varphi^{k,\pi}_{t',i+1}$ and train passing–passing arcs $\varphi^{k,\pi}_{t,i} \to \varphi^{k,\pi}_{t',i+1}$. When one of these arcs is selected ($x^{k,\pi}_{uv} = 1$), the other arcs cannot be selected.

$$\begin{array}{l}C^2_{it_1} = A \cap [\left\{\sigma^{k,\pi}_{t,i} \to \rho^{k,\pi}_{t',i+1,l} \middle| l = 1,2,\ldots m_{i+1}; t,t' = 0,1,\ldots,T; t_1 \le t \le t_1 + h_i - 1\right\} \\ \quad \cup \left\{\varphi^{k,\pi}_{t,i} \to \rho^{k,\pi}_{t',i+1,l} \middle| m'_{i+1} = 1; t,t' = 0,1,\ldots,T; t_1 \le t \le t_1 + h_i - 1\right\} \\ \quad \cup \left\{\sigma^{k,\pi}_{t,i} \to \varphi^{k,\pi}_{t',i+1} \middle| m'_i = 1; l = 1,2,\ldots m_{i+1}; t,t' = 0,1,\ldots,T; t_1 \le t \le t_1 + h_i - 1\right\} \\ \quad \cup \left\{\varphi^{k,\pi}_{t,i} \to \varphi^{k,\pi}_{t',i+1} \middle| m'_i = m'_{i+1} = 1; t,t' = 0,1,\ldots,T; t_1 \le t \le t_1 + h_i - 1\right\}]\end{array} \tag{14}$$

(c) Overtaking constraints

For any station i, overtaking is not allowed in the section $s_i \to s_{i+1}$. For each pair of different time points t_1 and t_2 ($t_1 < t_2$), let t be the moment when train k leaves from station s_i, and t_2 is the moment when train k reaches (including stop and pass) s_{i+1} station. t_1 is the time when the train k′ leaves from station i (including after stopping and passing through without stopping), and t' is the time when the train k′ reaches (including stopping and passing through) s_{i+1} station. For $s_i \to s_{i+1}$ section, if the train k leaves s_i earlier than k′ departure time t_1, in $t \in (t_1, t_2)$ within the open interval train k has incompatible constraint set $B_{it_1t_2}$; if train k′ arrives at s_{i+1} before the arrival time t_2 of train k, in $t' \in (t_2, T)$ half-open interval, train k′ has incompatible constraint set $B\prime_{it_1t_2}$. $B_{it_1t_2}$ and $B\prime_{it_1t_2}$ form the section prohibition of overtaking constraint arc set $C^3_{it_1t_2}$. When one of these arcs is selected ($x^{k,\pi}_{uv} = 1$), the other arcs cannot be selected.

$$\begin{aligned}
B_{it_1t_2} = A \cap [&\left\{\sigma^{k,\pi}_{t_1,i} \to \rho^{k,\pi}_{t_2,i+1,l} \middle| l = 1,2,\ldots m_{i+1}; t_1 < t < t_2\right\} \\
&\cup\left\{\sigma^{k,\pi}_{t,i} \to \varphi^{k,\pi}_{t_2,i+1} \middle| m'_{i+1} = 1; t_1 < t < t_2\right\} \\
&\cup\left\{\varphi^{k,\pi}_{\mathrm{t,i}} \to \rho^{k,\pi}_{t_2,i+1,l} \middle| m'_i = 1; l = 1,2,\ldots m_{i+1}; t_1 < t < t_2\right\} \\
&\cup\left\{\varphi^{k,\pi}_{\mathrm{t,i}} \to \varphi^{k,\pi}_{t_2,i+1} \middle| m'_i = m'_{i+1} = 1; t_1 < t < t_2\right\}] \\
B'_{it_1t_2} = A \cap [&\left\{\sigma^{k,\pi}_{t_1,i} \to \rho^{k,\pi}_{t',i+1,l} \middle| l = 1,2,\ldots m_{i+1}; t_2 < t' \le T\right\}k \\
&\cup\left\{\sigma^{k,\pi}_{t_1,i} \to \varphi^{k,\pi}_{t',i+1} \middle| m'_{i+1} = 1; t_2 < t' \le Tvk\right. \\
&\cup\left\{\varphi^{k,\pi}_{t_1,i} \to \rho^{k,\pi}_{t',i+1,l} \middle| m'_i = 1; l = 1,2,\ldots m_{i+1}; t_2 < t' \le T\right\}^{t,} \\
&\cup\left\{\varphi^{k,\pi}_{t_1,i} \to \varphi^{k,\pi}_{t',i+1} \middle| m'_i = m'_{i+1} = 1; t_2 < t' \le T\right\}] \\
&C^3_{it_1t_2} = B_{it_1t_2} \cup B'_{it_1t_2}
\end{aligned} \tag{15}$$

(d) Platform track exclusive constraint

For any side track l of any station s_i, it can be occupied by at most one train at a time. Let t be the time when the train starts to stop at l track of station i, t' is the time when the train finishes stopping at l track of station i, $t_1 - 1$ is the time when the train starts to wait at l track of station i and t_1 is the time when the train finishes waiting at l track of station i. Then, for any time t_1 of the track l at station i, there is a set of incompatible constraints $C^4_{it_1}$ in the closed interval $t_1 \in [t, t']$. The collection includes two kinds of spatial-temporal arcs, stop arc $\rho^{k,\pi}_{t,i,l} \to \overline{\rho}^{k,\pi}_{t',i,l}$ and waiting arc $\overline{\rho}^{k,\pi}_{t_1-l,i,l} \to \overline{\rho}^{k,\pi}_{t_1,i,l}$, respectively. When one of these arcs is selected ($x^{k,\pi}_{uv} = 1$), the other arcs cannot be selected.

$$C^4_{ilt_1} = A \cap \left[\left\{\rho^{k,\pi}_{t,i,l} \to \overline{\rho}^{k,\pi}_{t',i,1} \mid t \le t_1 \le t'\right\} \cup \left\{\overline{\rho}^{k,\pi}_{t_1-1,i,l} \to \overline{\rho}^{k,\pi}_{t_1,i,l}\right\}\right] \tag{16}$$

2.4. Decomposition Algorithm Based on Hybrid Heuristic Lagrangian Relaxation (HHLR)

The decision variables y_π and pl_π determine the second part (i.e., the supply–demand satisfaction degree) of Equation (2), and the variable $x^{k,\pi}_{uv}$ determines the first part (i.e., the running time and energy consumption) of Equation (2). The proposed algorithm takes these three variables as two groups, where y_π and pl_π are group 1 and $x^{k,\pi}_{uv}$ is group 2, then uses a heuristic framework to optimize the first group and the Lagrangian relaxation to optimize the second group.

2.4.1. Optional Set-Based Algorithm Framework

For ensuring that the resulting multi-cycle train timetable can meet the passenger demand while being easy for passengers to remember, this paper constructs a candidate set of lines with optional cycle lengths (i.e., 30 min, 40 min, and 60 min, which are convenient for passengers to remember) and uses random search to solve the model. Such optional set-based algorithm framework is shown in Figure 2. In step 1, basic information of line, passenger demand and parameters of timetable are input. In step 2, the model selects a set

of line from the input lines randomly, which determines the value of y_πs. Then, for each selected line, select a cycle length from the optional cycle lengths, which determines the value of pl_πs. In step 3, solve the MTSDE model and obtain feasible solution. Store the solution into the result set. This process repeats N_i times, and in the final step, we select the solution with the best objective value as the final solution.

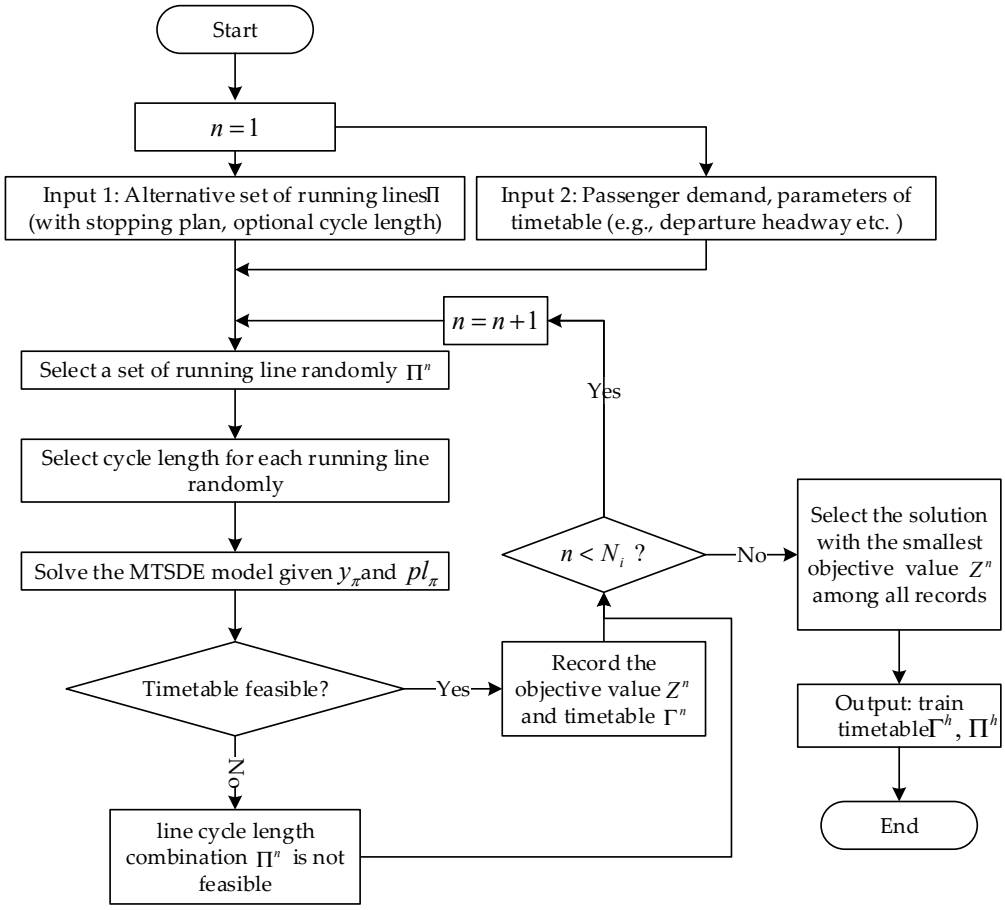

Figure 2. Solution framework based on alternative set.

The previously mentioned step 3 requires solving the difficult problem caused by complex spatial-temporal constraints in Equations (3)–(8). We use the idea of Lagrangian decomposition for the optimization.

2.4.2. Decomposition of the Original MTSDE Model

By using Lagrangian decompoition method, the original problem can be decomposed into a lower bound problem and can be decomposed into about $|K|$-independent shortest path problem $LRP(K)$. The upper bound heuristic algorithm is used to solve the upper bound solution, and the Lagrange operator is updated according to the upper and lower bound solution, and the optimal solution is obtained by continuing the iteration.

Two termination conditions are used to stop the Lagrangian decomposition algorithm. One is that the maximum number of iterations M_L is reached. The other is that the lower bound objective function value LB, corresponding to the relaxation problem, and the upper bound objective function value UB are satisfied: $Gap = \frac{(UB-LB)}{LB} \cdot 100\% \leq \delta_L$. The basic process of Lagrange decomposition algorithm is shown in Algorithm 1 (Algorithm process for solving the model).

Algorithm 1 Lagrangian Decomposition Algorithm

Lagrangian Relaxation: According to the Lagrange relaxation of the original integer programming problem P, the corresponding relaxation problem $\widetilde{P}(\lambda)$ is obtained.
Problem decomposition: Relaxation problem $\widetilde{P}(\lambda)$ is decomposed into about |K| independent of the shortest path problem $\widetilde{P}_k(\lambda)$.
Initialize: In order to solve the train schedule problem $\widetilde{P}_k(\lambda)$, let the initial iteration number $t = 1$, the corresponding Lagrange multiplier $\lambda^1 = 0$, the upper bound objective function value is $UB = +\infty$, and the lower bound objective function value is $LB = -\infty$
while $t \leq M_L$ or $Gap \geq \delta_L$ **then**
  According to the current Lagrange multiplier, the problem $\widetilde{P}_k(\lambda)$ with constraints is solved using dynamics programming algorithm and obtains the lower bound solution X^t_{LB}.
  Calculate the objective function value LB^t of $\widetilde{P}(\lambda)$ problem corresponding to the lower bound solution X^t_{LB}.
  if $LB^t > LB$ **then**
    Update the optimal lower bound solution, let $LB = LB^t, X_{LB} = X^t_{LB}$.
  end if
  The upper bound solution X^t_{UB} is obtained by using the greedy algorithm for X^t_{LB}.
  Compute the objective function value UB^t of the P problem corresponding to the upper bound solution X^t_{UB}.
  if $UB^t < UB$ **then**
    Update the optimal upper bound solution, let $UB = UB^t, X_{UB} = X^t_{UB}$
  end if
  Lagrange multipliers are updated by sub gradient method.
  $t = t + 1$
  $Gap = (UB - LB)/LB \cdot 100\%$
end while
return UB

The network is transformed into the minimum cost of train occupancy of network arcs. $G_k = (V_k,\ A_k)$ is the spatial-temporal subnetwork corresponding to train k, V_k is the set of spatial-temporal nodes that can be occupied by train k and A_k is the set of spatial-temporal arcs that can be occupied by train k.

Relax the complicated constraint (6) of the original problem and introduce $\lambda_C \geq 0$ to construct the Lagrangian relaxation dual problem $\widetilde{P}(\lambda)$, where λ is the vector of λ_C value, λ_C is the Lagrange multiplier of constraint (6).

$$\begin{aligned}\widetilde{P}(\lambda):\ Min \sum_{k\in K}\sum_{u\to v\in A^k}\left(\xi^k_t(u,v)+\rho_1\xi^k_e(u,v)\right)\cdot x^{k,\pi}_{uv}+\textstyle\sum_{c\in C}\lambda_C\left(\sum_{\pi\in\Pi}\sum_{k\in K}\sum_{u\to v\in c}x^{k,\pi}_{uv}-1\right)\\ +\rho_2\sum_{i\in S}\sum_{m\in M}\left(\textstyle\sum_{t\in[ts_m,te_m]}\delta^i_t-\sum_{t\in[ts_m,te_m]}\sum_{\pi\in\Pi}y_\pi\cdot\frac{T}{pl_\pi\cdot m}\cdot\sigma^\pi_i\right)^2\end{aligned} \tag{17}$$

$$\textstyle\sum_{\pi\in\Pi}\sum_{\{v:\widetilde{o}\to v\in A^k\}}x^{k,\pi}_{\widetilde{o}v}=1,\forall k\in K \tag{18}$$

$$\textstyle\sum_{\pi\in\Pi}\sum_{\{u:u\to\overline{d}\in A^k\}}x^{k,\pi}_{u\overline{d}}=1,\forall k\in K \tag{19}$$

$$\textstyle\sum_{\{u:u\to v\in A^k\}}x^{k,\pi}_{uv}=\sum_{\{w:v\to w\in A^k\}}x^{k,\pi}_{vw},\forall\pi\in\Pi,\forall k\in K_\pi;v\in V^k\backslash\left\{\overline{O},\overline{d}\right\} \tag{20}$$

$$x^{w_\pi,\pi}_{uv:(i,t)\to(j,t')}=x^{k,\pi}_{uv:(i,t_1)\to(j,t_2)}\forall\pi\in\Pi,k\in K_\pi,q^k_\pi>1 \tag{21}$$

$$t_1=t+\left(q^k_\pi-1\right)\cdot pl_\pi,t_2=t'+\left(q^k_\pi-1\right)\cdot pl_\pi\quad\forall i,j\in E,\ \forall t,t'\in T \tag{22}$$

$$\sum_{v\in V_k}a_{kv}+a'_k\left(\sum_{u\to v\in A^k}x^{k,\pi}_{uv}-1\right)+a''_k\left(\sum_{u\to v\in A^k}x^{k,\pi}_{uv}-1\right)\leq\eta,\ \forall\pi\in\Pi,k\in K_\pi \tag{23}$$

$$x^{k,\pi}_{uv}\in\{0,1\},\forall\pi\in\Pi,k\in K_\pi;u\to v\in A^k \tag{24}$$

2.4.3. Lower Bound Solution Algorithm of Lagrangian Sub-Problem Based on Dynamic Programming Algorithm

For each train, suppose $G_k = (N_k, A_k)$ is the spatial-temproal network corresponding to train k, N_k is the set of spatial-temporal nodes that train k can occupy and A_k is the set of spatial-temporal arcs that train k can use. Each train $k \in K$ has a Lagrangian sub-problem $\widetilde{P}_k(\lambda)$. In this objective function, the difference between the station passenger demand and the train supply is a constant. Thus, this part is ignored in the objective function of $\widetilde{P}_k(\lambda)$.

$$\widetilde{P}_k(\lambda): Min \sum_{u \to v \in A^k} \left(\xi_t^k(u,v) + \rho_1 \xi_e^k(u,v)\right) x_{uv}^{k,\pi} + \sum_{c \in C} \lambda_C \left(\sum_{\pi \in \Pi} \sum_{u \to v \in c} x_{uv}^{k,\pi} - 1\right) \tag{25}$$

$$\sum_{\pi \in \Pi} \sum_{\{v:\widetilde{o} \to v \in A^k\}} x_{\widetilde{o}v}^{k,\pi} = 1, \forall k \in K \tag{26}$$

$$\sum_{\pi \in \Pi} \sum_{\{u:u \to \overline{d} \in A^k\}} x_{u\overline{d}}^{k,\pi} = 1, \forall k \in K \tag{27}$$

$$\sum_{\{u:u \to v \in A^k\}} x_{uv}^{k,\pi} = \sum_{\{w:v \to w \in A^k\}} x_{vw}^{k,\pi}, \forall \pi \in \Pi, \forall k \in K_\pi; v \in V^k \backslash \left\{\overline{O}, \overline{d}\right\} \tag{28}$$

$$x_{uv:(i,t) \to (j,t')}^{w_\pi,\pi} = x_{uv:(i,t_1) \to (j,t_2)}^{k,\pi} \forall \pi \in \Pi, k \in K_\pi, q_\pi^k > 1 \tag{29}$$

$$t_1 = t + \left(q_\pi^k - 1\right) \cdot pl_\pi, t_2 = t' + \left(q_\pi^k - 1\right) \cdot pl_\pi \quad \forall i,j \in E, \forall t,t' \in T \tag{30}$$

$$\sum_{v \in V_k} a_{kv} + a_k' \left(\sum_{u \to v \in A^k} x_{uv}^{k,\pi} - 1\right) + a_k'' \left(\sum_{u \to v \in A^k} x_{uv}^{k,\pi} - 1\right) \le \eta, \forall \pi \in \Pi, k \in K_\pi \tag{31}$$

It is easy to obtain $A_{\text{dep}} \cap c = \varnothing$ for all $c \in \mathcal{C}$ from the definitions for incompatibility arcs. We can obtain $\sum_{\{C \in C:u \to v \in C\}} \lambda_C = 0$. Thus, the weights of different arcs can be deduced by Equation (32).

$$\delta_{uv}^k = \begin{cases} \xi_t^k(u,v) + \rho_1 \xi_e^k(u,v), & \text{otherwise} \\ \xi_t^k(u,v) + \rho_1 \xi_e^k(u,v) + \sum\limits_{[c \in C:u \to v \in C]} \lambda_C, & if\ u \to v \in A_{trv} \end{cases} \tag{32}$$

After the above derivation, each sub-problem $\widetilde{P}_k'(\lambda)$ is a shortest path problem with weight δ_{uv}^k. Thus, each sub-problem is transformed into a minimum cost network flow problem which is from $\overline{o}$ to $\overline{d}$. Because G_k is a cyclic network, $\widetilde{P}_k'(\lambda)$ can be solved effectively through a standard dynamic programming algorithm [39].

Suppose Z^* is the optimal objective value of original problem P. Suppose $L(\lambda)$ indicates the optimal objective value of lower bound problem $\widetilde{P}_k(\lambda)$. For any nonnegative vector λ, $L(\lambda)$ is a lower bound Z^*.

2.4.4. Upper Bound Solution of Lagrangian Sub-Problem Based on Heuristic Algorithm

After solving the relaxation problem, then lower bound solution x_{LB} of problem P can be obtained. x_{LB}. In the lower bound solution, there may exist conflicts, and the objective function of the lower bound solution will be better than the actual optimal solution. Although the lower bound solution cannot be directly used because it is not feasible, it can lead to the obtaining of feasible solutions. In order to ensure the feasibility of the solution, a heuristic algorithm is used for calculating upper bound solution. The basic process of the algorithm is shown in Algorithm 2 (Basic process of the greedy algorithm).

Algorithm 2 Greedy Algorithm

1: According to the results of the lower bound solution, the optimal objective values of the sub-problem $\widetilde{p}_k(\lambda)$s are sorted from small to large so that the train k with the smallest optimal objective is ranked first
2: The train's spatial-temporal path is arranged one by one, according to the sequence order, by solving the shortest path
3: Search all feasible paths to find the shortest path of the train. The network G_k does not contain any arc that is incompatible with the arc passed by the last train by eliminating arcs who violate the arrival headway, departure headway constraints, etc.
4: Output: a set of $x_{uv}^{k,\pi}$ values of all $k \in K$, $\pi \in \Pi$ and $u \to v \in A$, obtain all train paths.

2.4.5. The Updates of Lagrangian Multipliers

We use the subgradient algorithm to update the λ. The update is shown in Equations (33)–(35).

$$\lambda^m \leftarrow \max\left\{\lambda^m + \theta \cdot \frac{UB - L(\lambda,\mu)}{\| \chi \|^2} \cdot \chi^m, 0\right\} (m = 1, 2, \ldots, |\mathcal{C}|) \tag{33}$$

where $L(\lambda,\mu)$ is the optimal value of solution of $\widetilde{P}(\lambda,\ \mu)$. $\theta > 0$ is the preset length. UB represents the current optimal solution of P. For $m = 1, 2, \ldots, |\mathcal{C}| + \left|A_{de}^{k,\pi} \cup A_{trv}^{k,\pi}\right|$, χ^m represents the mth element of vector χ. For $m = 1, 2, \ldots, |\mathcal{C}|$, the λ^m represents the mth element of vector λ.

We denote the $\chi(i)$ as the vector χ in *ith* iteration and used a modified subgradient method (Camerini et al. [40], Xu [41], Caprara [9]) to update χ, where we used $\widetilde{\chi}$ instead of χ. The process is shown in Equations (34) and (35).

$$\widetilde{\chi}^{(i)} \leftarrow \chi^{(i)} + b\widetilde{\chi}^{(i-1)} \tag{34}$$

$$b = \begin{cases} -a \cdot \frac{\widetilde{\chi}^{(i-1)} \cdot \chi^{(i)}}{||\widetilde{\chi}^{(i-1)}||^2}, & \text{if } \widetilde{\chi}^{(i-1)} \cdot \chi^{(i)} < 0 \\ 0, & \text{otherwise} \end{cases} \tag{35}$$

where a is a given scale and $0 \leq a \leq 2$.

3. Numerical Experiments

In order to verify the model and algorithm proposed in this paper, three cases were designed, including the model performance characteristics under different passenger flow scenarios, the calculation efficiency under different scale scenarios and the actual large passenger flow. Visual Studio 2019 and C# language are used to implement the model and algorithm proposed in this paper. The hardware platform is powered by an Intel Core i7 processor and 16 GB RAM. The operation system of the experiment platform is Windows 10. The upper limit of solving time is set to 1 h.

3.1. Experiment Designs

We chose a double-track railway corridor with 7 stations as the hypothetical railway network (Figure 3). The entire length of line is 166 km, and the design speed is 350 km/h.

Figure 3 shows the layout of selected directions, where station 1 is the origin station and stations 6 and station 7 are the destination stations. The minimum safety departure time interval is set to 4 min, the minimum safety arrival time interval is set to 3 min, and the acceleration and deceleration times for all trains are specified as 2 min and 3 min, respectively. The pure running times of all trains in sections are shown in Figure 3, and the station dwell time of all trains are set to 2–8 min. The planning time horizon of this case is 6:00–12:00; the time period for passenger demand is 6:00–11:00. Station 1 is the origin station, and the total time is divided into 5 segments based on 60 min. Table 3 shows the line plan of multi-cycle train timetable model of this case.

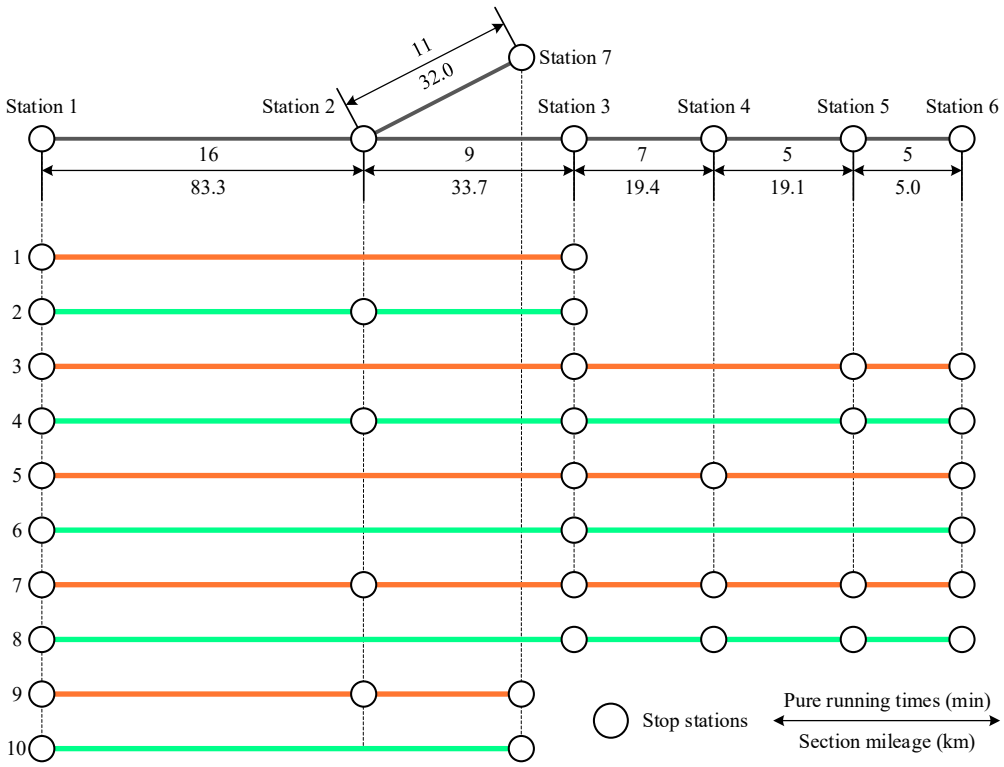

Figure 3. Railway network for experiments, where the colored lines represent optional lines.

Table 3. Lines in line plan.

Line	Origin	Destination	Route	Stop Plans (Intermediate Stations)	Optional Cycle
1	1	3	1→2→3	-	30, 40
2	1	3	1→2→3	2	30, 40, 60, 90
3	1	6	1→2→3→4→5→6	3, 5	30, 40, 60, 90
4	1	6	1→2→3→4→5→6	2, 3, 5	60, 90, 120, 150, 180
5	1	6	1→2→3→4→5→6	3, 4	60, 90, 120, 150, 180, 240, 300, 360, 420, 480, 540, 600, 660, 720, 780, 840, 900, 960
6	1	6	1→2→3→4→5→6	3	60, 90, 120, 150, 180, 240, 300, 360, 420, 480, 540, 600, 660, 720, 780, 840, 900, 960, 1020
7	1	6	1→2→3→4→5→6	2, 3, 4, 5	60, 90, 120, 150, 180, 240, 300, 360, 420, 480, 540, 600, 660, 720, 780, 840, 900, 960
8	1	6	1→2→3→4→5→6	3, 4, 5	60, 90, 120, 150, 180, 240, 300, 360, 420, 480, 540, 600, 660, 720, 780, 840, 900, 960, 1020
9	1	7	1→2→7	2	60, 90, 120, 150, 180, 240, 300, 360, 420, 480, 540, 600, 660, 720, 780, 840, 900, 960, 1020
10	1	7	1→2→7	-	30, 40, 50

All stations (station 1 to station 7) are served and set $\rho_1 = 0.005$ and $\rho_2 = 1.0$. The solution of the model is based on Gurobi 9.5.2 and C# on the Visual Studio 2022 platform.

3.2. Comparison of Single-Cycle and Multi-Cycle Train Timetable under Different Scenarios

There are three different scenarios of the passenger flow demand. Scenario 1 is characterized by two passenger flow peaks. Scenario 2 is characterized by one passenger flow peak. Scenario 3 is characterized by a passenger flow without peaks. For these three

types of passenger flow distributions, the corresponding multi-cycle train timetable is obtained according to the multi-cycle train timetable optimization model proposed in this paper, and the single-cycle train timetable is obtained at the same time. The metrics are compared between the multi-cycle train timetable and the single-cycle train timetable. The corresponding metrics include the objective function value, satisfaction ratio of passenger demand, train vacancy rate, running time and energy consumption.

During the demand period, the supply of trains in each period should match the demand of the passenger flow to ensure the regular operation of the trains and meet the travel demand of the passengers in different periods. In order to verify the matching degree between the multi-cycle train diagram and the time distribution of the passenger flow demand as well as the performance of the multi-cycle train diagram model, the corresponding multi-cycle and single-cycle train timetable are solved, respectively, and the corresponding metrics are compared.

The cycle length of the train lines in the single-cycle train timetable model is set to 60 min.

3.2.1. Scenario 1 with Two Passenger Flow Peaks

The train diagrams of the single-cycle train timetable model and the multi-cycle train timetable model of passenger flow distribution 1 are shown in Figure 4. It can be seen from the multi-cycle train timetable that the number of train departures during the two peak periods is larger than the number of the off-peak period (i.e., in the peak period from 6 a.m. to 8 a.m., there are 11 trains departing from the terminal station, while in the off-peak period from 8 a.m. to 10 a.m., there are only 7 trains departing from the terminal station), while the number of train departures in each period of the single-cycle train timetable is the same.

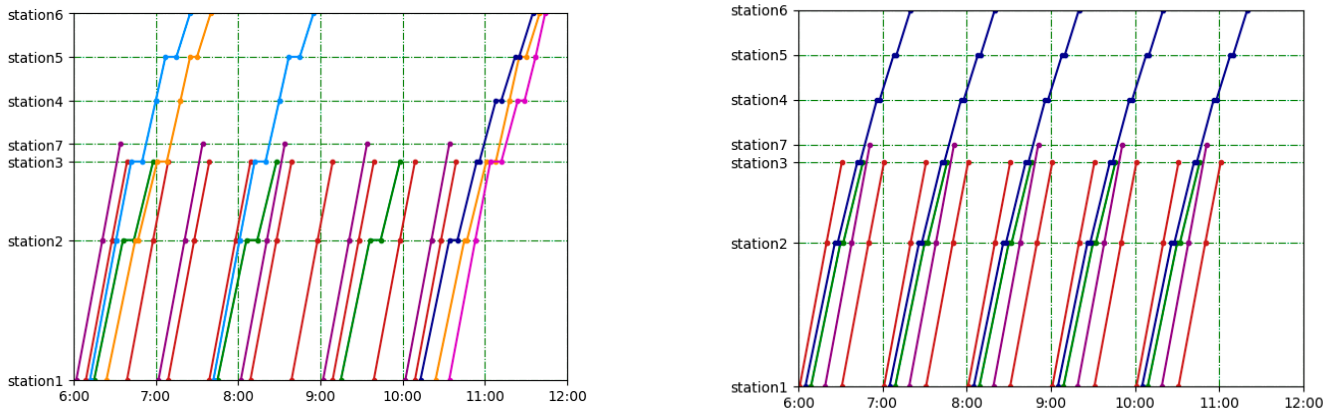

Figure 4. Multi-cycle train timetable and single-cycle train timetable under scenario 1. (**a**) Multi-cycle train timetable. (**b**) Single-cycle train timetable. Red, green, blue, orange, violet, navy blue and purple represents Line 1, 2, 3, 4, 5, 7 and 10 in Table 3, respectively.

The matching results of the two train timetables and the passenger flow are shown in Figure 5 (the sum of the supply and demand of all the stations during each time duration, i.e., S_o includes all stations), and the details of the supply and demand matching degree can be seen in Tables 4 and 5.

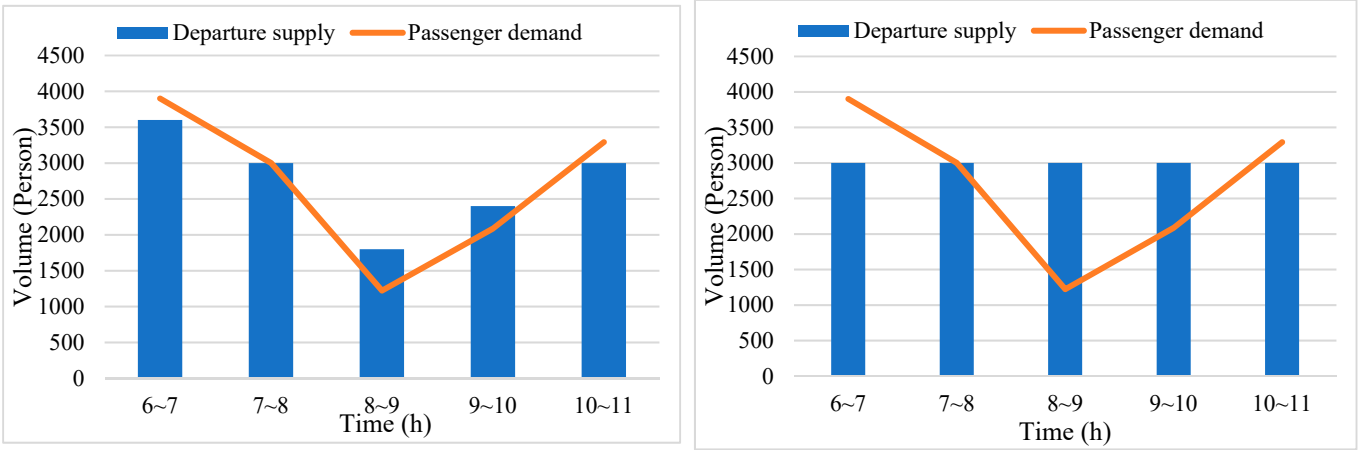

Figure 5. Supply and demand matching diagram under scenario 1. (**a**) Supply and demand matching diagram of multi-cycle train timetable. (**b**) Supply and demand matching diagram of single-cycle train timetable.

Table 4. Details of supply and demand matching degree of multi-cycle timetable in scenario 1.

Figure 4a	**6~7**	**7~8**	**8~9**	**9~10**	**10~11**
Departure supply	3600	3000	1800	2400	3000
Passenger demand	3901	3001	1223	2088	3293
SDMD *	92.57%	99.97%	62.39%	86.12%	91.49%

* SDMD (supply and demand matching degree): $EXP\left(-\frac{|Passenger\ demand - Departure\ supply|}{Passenger\ demand}\right) \cdot 100\%$.

Table 5. Details of supply and demand matching degree of single-cycle timetable in scenario 1.

Figure 4b	**6~7**	**7~8**	**8~9**	**9~10**	**10~11**
Departure supply	3000	3000	3000	3000	3000
Passenger demand	3901	3001	1223	2088	3293
SDMD *	79.38%	99.97%	23.39%	64.61%	91.49%

* SDMD (supply and demand matching degree): $EXP\left(-\frac{|Passenger\ demand - Departure\ supply|}{Passenger\ demand}\right) \cdot 100\%$.

It can be seen from the supply–demand matching graph that, as the time changes, the change trend of the departure frequency of the multi-cycle train timetable is more in line with the change trend of the passenger demand. Specifically, the supply and demand matching degrees in all the time periods in the multi-cycle train timetable exceed 60%, with an average value of 86.51%, which is only 71.77% in the single-cycle train timetable. In terms of the energy consumption, line 1 in the multi-cycle train timetable has the highest energy consumption, while line 3 in the single-cycle train timetable has the highest energy consumption (Table 6).

Table 6. Energy consumption of all lines in scenario 1 (kwh).

	Line (Line Color)						
	1 (Red)	**2 (Green)**	**3 (Blue)**	**4 (Orange)**	**5 (Violet)**	**7 (Navy blue)**	**10 (Purple)**
MT *	59,168.79	23,362.32	26,286.6	28,712.86	13,143.3	16,300.63	35,308.45
ST	65,743.1	38,937.2	77,847.8	-	-	-	35,308.45

* MT: Multi-cycle train timetable. ST: Single-cycle train timetable.

The corresponding data metrics are shown in Table 7. According to the metrics, because the single-cycle train timetable should keep the same train departure frequency in each cycle, the single-cycle timetable could not adapt to the different passenger flow

demand in the different periods. The demand satisfaction ratio of the single-cycle train timetable is 4.44% lower than that of the multi-cycle train timetable. Meanwhile, the train vacancy rate of the single-cycle train timetable is higher, which indicates that the single-cycle train timetable could not meet the passenger flow demand as well as the multi-cycle train timetable. The total energy consumption of the multi-cycle train timetable is 15,553.6 kwh lower than the single-cycle train timetable.

Table 7. Comparison of metrics in scenario 1.

	Total Number of Trains Running	The Number of Passenger Demand	Demand Satisfaction Ratio	Train Vacancy Rate	Running Time (h)	Energy Consumption (kwh)
MT *	25	12,911	95.59%	6.44%	14.33	202,282.95
ST	25	12,311	91.15%	17.93%	17.57	217,836.55

* MT: Multi-cycle train timetable. ST: Single-cycle train timetable.

3.2.2. Scenario 2 with One Passenger Flow Peaks

The solution results of the single-cycle train timetable and the multi-cycle train timetable of passenger flow distribution 2 are shown in Figure 6. The matching results of the two timetables and passenger flow are shown in Figure 7, and the corresponding data metrics are shown in Tables 8 and 9.

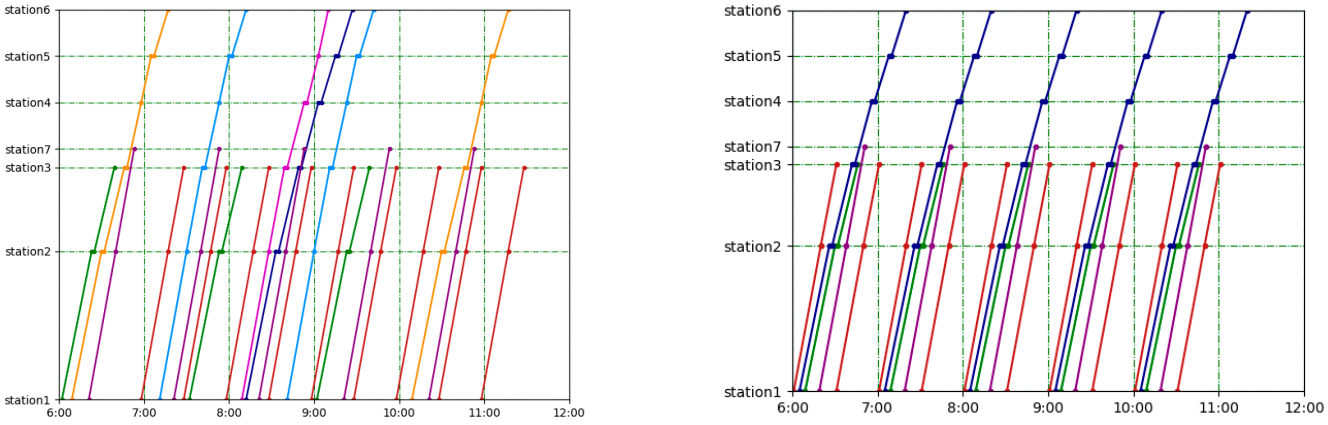

Figure 6. Multi-cycle train timetable and single-cycle train timetable under scenario 2. (**a**) Multi-cycle train timetable. (**b**) Single-cycle train timetable. Red, green, blue, orange, violet, navy blue and purple represents Line 1, 2, 3, 4, 5, 7 and 10 in Table 3, respectively.

It can be seen from the multi-cycle train timetable that the number of train departures during the peak period is significantly larger than that during the off-peak period, while the number of train departures in each period of the single-cycle train timetable is the same. It can be seen from the supply–demand matching diagram that the supply–demand matching degree of the multi-cycle train timetable is also better than that of the single-cycle train timetable. Specifically, it can be seen from Tables 8 and 9 that the supply and demand matching degrees in all the time periods in the multi-cycle train timetable exceed 85%, with an average value of 90.15%, which is only 78.54% in the single-cycle train timetable. It is also clear that the single-peak flows in scenario 2 have a higher matching ratio between the supply and demand than the double-peak flows in scenario 1.

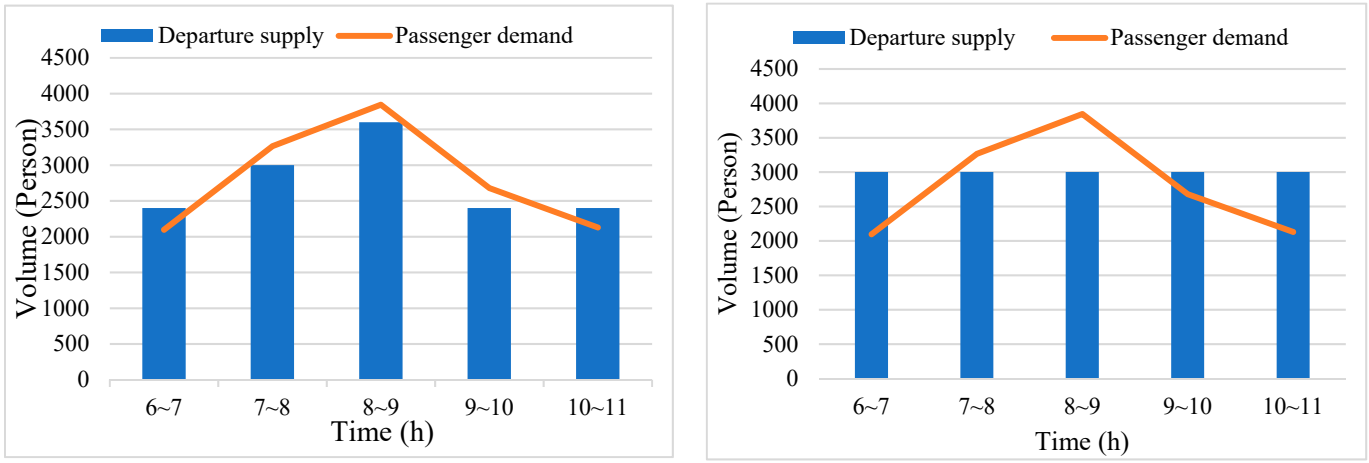

Figure 7. Supply and demand matching diagram under scenario 2. (**a**) Supply and demand matching diagram of multi-cycle train timetable. (**b**) Supply and demand matching diagram of single-cycle train timetable.

Table 8. Details of supply and demand matching degree of multi-cycle timetable in scenario 2.

Figure 6a	6~7	7~8	8~9	9~10	10~11
Departure supply	2400	3000	3600	2400	2400
Passenger demand	2097	3266	3845	2680	2130
SDMD *	86.55%	92.18%	93.83%	90.08%	88.09%

* SDMD (supply and demand matching degree): $EXP\left(-\frac{|Passenger\ demand - Departure\ supply|}{Passenger\ demand}\right) \cdot 100\%$.

Table 9. Details of supply and demand matching degree of single-cycle timetable in scenario 2.

Figure 6b	6~7	7~8	8~9	9~10	10~11
Departure supply	3000	3000	3000	3000	3000
Passenger demand	2097	3266	3845	2680	2130
SDMD *	65.01%	92.18%	80.27%	88.75%	66.47%

* SDMD (supply and demand matching degree): $EXP\left(-\frac{|Passenger\ demand - Departure\ supply|}{Passenger\ demand}\right) * 100\%$.

In terms of the energy consumption, similar to scenario 1, line 1 in the multi-cycle train timetable has the highest energy consumption, while line 3 in the single-cycle train timetable has the highest energy consumption (Table 10).

Table 10. Total energy consumption of all lines under scenario 2 (kwh).

	Line (Line Color)						
	1 (Red)	**2 (Green)**	**3 (Blue)**	**4 (Orange)**	**5 (Violet)**	**7 (Navy blue)**	**10 (Purple)**
MT *	59,168.79	-	26,286.6	28,712.86	13,143.3	15,569.56	35,308.45
ST	65,743.1	38,937.2	77,847.8	-	-	-	35,308.45

* MT: Multi-cycle train timetable. ST: Single-cycle train timetable.

It can be seen from the data in Table 11 that the single-cycle train timetable demand satisfaction ratio is lower than that of the multi-cycle train timetable. At the same time, the train vacancy rate is higher, indicating that the single-cycle train timetable is much less satisfying than the multi-cycle train timetable. For the passenger flow distribution 2, the running time of the multi-cycle train timetable is 2.32 h lower than that of the single-cycle train timetable, and the total energy consumption of the multi-cycle train timetable is 16,284.67 kwh lower than the single-cycle train timetable.

Table 11. Comparison of metrics under scenario 2.

	Total Number of Trains Running	The Number of Passenger Demand	Demand Satisfaction Ratio	Train Vacancy Rate	Running Time (h)	Energy Consumption (kwh)
MT *	25	13,227	94.36%	4.15%	14.63	201,551.88
ST	25	14,618	92.07%	13.95%	16.95	217,836.55

*MT: Multi-cycle train timetable. ST: Single-cycle train timetable.

3.2.3. Scenario 3 without Passenger Flow Peaks

The solution results of the single-cycle train timetable and the multi-cycle train timetable of passenger flow distribution 3 are shown in Figure 8. The matching results of the two timetables and passenger flow are shown in Figure 9, and the corresponding data metrics are shown in Tables 12 and 13.

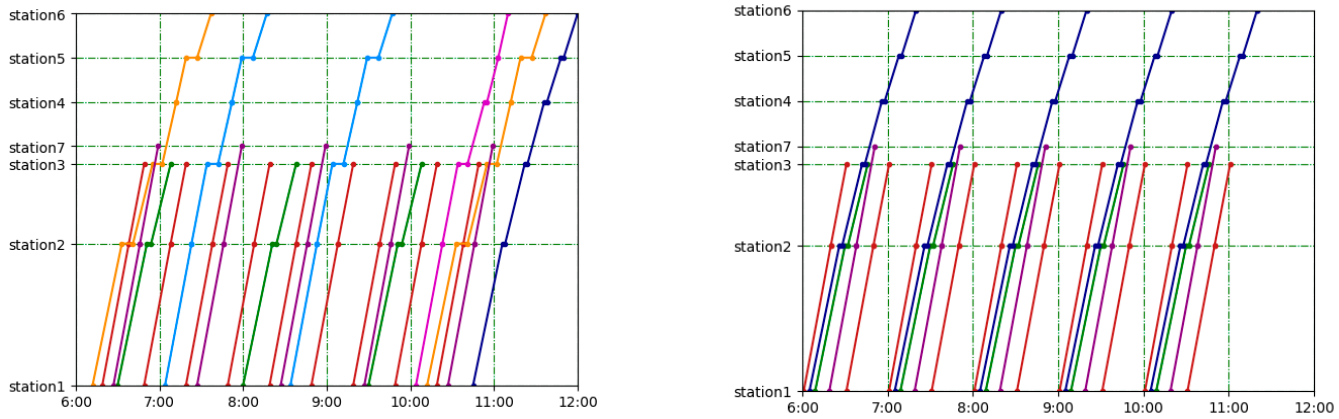

Figure 8. Multi-cycle train timetable and single-cycle train timetable under scenario 3. (a) Multi-cycle train timetable. (b) Single-cycle train timetable. Red, green, blue, orange, violet, navy blue and purple represents Line 1, 2, 3, 4, 5, 7 and 10 in Table 3, respectively.

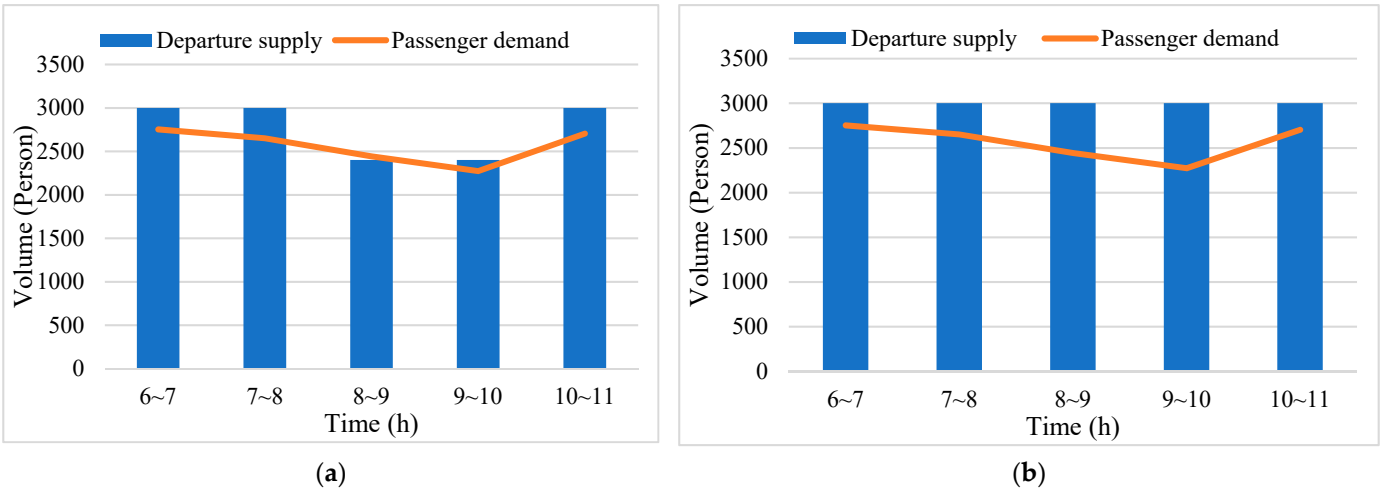

Figure 9. Supply and demand matching diagram under scenario 3. (**a**) Supply and demand matching diagram of multi-cycle train timetable. (**b**) Supply and demand matching diagram of single-cycle train timetable.

Table 12. Details of supply and demand matching degree of multi-cycle timetable in scenario 3.

Figure 8a	6~7	7~8	8~9	9~10	10~11
Departure supply	3000	3000	2400	2400	3000
Passenger demand	2753	2651	2443	2273	2704
SDMD *	91.42%	87.66%	98.26%	94.57%	89.63%

* SDMD (supply and demand matching degree): $EXP\left(-\frac{|Passenger\ demand-Departure\ supply|}{Passenger\ demand}\right)*100\%$.

Table 13. Details of supply and demand matching degree of single-cycle timetable in scenario 3.

Figure 8b	6~7	7~8	8~9	9~10	10~11
Departure supply	3000	3000	3000	3000	3000
Passenger demand	2753	2651	2443	2273	2704
SDMD *	91.42%	87.66%	79.61%	72.63%	89.63%

* SDMD (supply and demand matching degree): $EXP\left(-\frac{|Passenger\ demand-Departure\ supply|}{Passenger\ demand}\right)*100\%$.

It can be seen from the supply–demand matching graph and that the metrics of the multi-cycle timetable and the single-cycle timetable have little change, indicating that for the passenger flow distribution with a stable passenger flow distribution, the multi-cycle train timetable can also meet the passenger flow demand. Specifically, it can be seen from Tables 12 and 13 that the supply and demand matching degrees in all the time periods in the multi-cycle train timetable exceed 85%, with an average value of 92.31%, which is only 84.19% in the single-cycle train timetable. It can be seen that the no-passenger flow peaks scenario has a better match between the supply and demand than the scenarios with peaks (scenario 1 and scenario 2).

In terms of the energy consumption, similar to scenario 1 and scenario 2, line 1 in the multi-cycle train timetable has the highest energy consumption, while line 3 in the single-cycle train timetable has the highest energy consumption (Table 14).

Table 14. Total energy consumption of all lines under scenario 3 (kwh).

	Line (Line Color)						
	1 (Red)	**2 (Green)**	**3 (Blue)**	**4 (Orange)**	**5 (Violet)**	**7 (Navy blue)**	**10 (Purple)**
MT *	59,168.79	23,362.32	28,214.84	29,676.98	13,143.3	15,569.56	35,308.45
ST	65,743.1	38,937.2	77,847.8	-	-	-	35,308.45

* MT: Multi-cycle train timetable. ST: Single-cycle train timetable.

From Table 15, we can see that the single-cycle train timetable demand satisfaction ratio is higher than that of the multi-cycle train timetable, which is different from the previous two scenarios. However, the train vacancy rate of the single-cycle train timetable is far higher than the multi-cycle train timetable. For the passenger flow distribution 3, the running time of the multi-cycle train timetable is 2.32 h lower than that of the single-cycle train timetable. In addition, the total energy consumption of the multi-cycle train timetable is 13,392.31 kwh lower than the single-cycle train timetable.

Table 15. Comparison of metrics under scenario 3.

	Total Number of Trains Running	The Number of Passenger Demand	Demand Satisfaction Ratio	Train Vacancy Rate	Running Time (h)	Energy Consumption (kwh)
MT *	25	12,781	99.7%	7.38%	14.34	204,444.24
ST	25	12,824	100%	14.51%	16.58	217,836.55

* MT: Multi-cycle train timetable. ST: Single-cycle train timetable.

3.3. Analysis of Solution Efficiency

The line plan in Section 3.1 and the passenger flow scenario in Section 3.2.1 are applied in this analysis. The time horizons in this analysis are set to 5 h, 10 h, 15 h, 20 h and 25 h. According to the comparison of the different cases in Table 16, the solution could be concluded that the objective function values are increasing along with the scale increasing (mainly influenced by the numbers of train departures and the energy consumption). Meanwhile, during the experiments of the small-scale case, the proposed algorithm performs similarly to the Gurobi solver as the accuracies in cases 1–3 range between 99.50% and 100%. However, the proposed algorithm works more efficiently than the Gurobi with the accuracy slightly decreasing. As shown in Figure 10, with the increase in the case scale, the proposed algorithm could finish the computing task within 200 s, while the Gurobi solvers need more than 2000 s.

Table 16. Comparison table of algorithm efficiency and accuracy for different cases.

Case ID	Time Horizons	Number of Trains	Algorithm Calculation Time Consumption (s)	The Objective Function Values Calculated by the Algorithm	Gurobi Calculation Time Consumption (s)	The Objective Function Values Calculated by Gurobi	Accuracy (%)
1	5	25	76	3475.21	92	3475.21	100.00%
2	10	50	152	6359.64	207	6353.28	99.90%
3	15	75	224	10,112.87	359	10,062.31	99.50%
4	20	100	299	13,727.10	890	13,521.19	98.48%
5	25	150	458	20,816.54	2093	20,192.04	96.91%

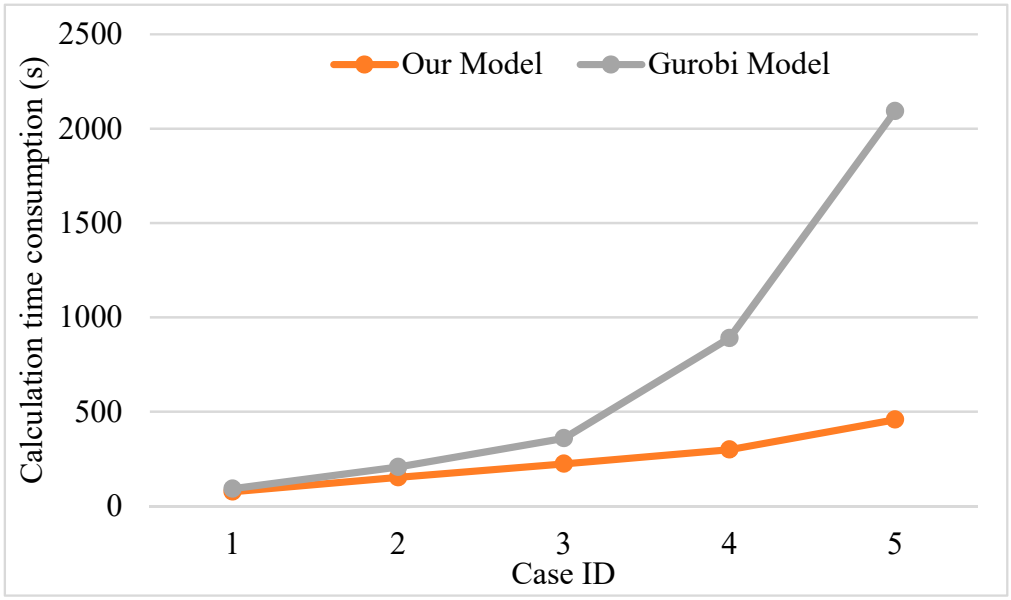

Figure 10. Solving time comparison.

3.4. Experiment Based on Real-World Case

The time and space range of the train diagram used in this case is 6:00–23:00. In terms of the passenger demand, the total period of the passenger demand considered is 6:00–22:00, which means that the period when the train departs from station *a* is 6:00–22:00, and the total time horizon is divided into 16 segments according to the time interval of 60 min. The set of the cycle alternatives for lines 1–8 (the passenger flow and operation lines associated with station 7 are not considered in this case) is shown in Table 3.

It can be seen from Figure 11 that the supply level of each time period of the obtained train operation diagram changes with the change in the passenger flow demand, which can

satisfy the passenger flow demand of each time period to a large extent. From Tables 17 and 18, we can see the distribution of the supply and demand matching under each time period. Specifically, the supply–demand matching degree is 91.16% during the morning peak period (7:00–8:00) and 92.38% during the evening peak period (19:00–20:00), which means that the model could satisfy the passenger flow demand effectively. Among them, the highest supply and demand matching degree is 94.52% during 10:00–11:00, while the lowest supply and demand matching degree is 84.16% throughout the whole day. To a large extent, it can meet the passenger flow demand at different times throughout the day. At the same time, the matching of the supply and demand also indicates that the model in this paper can obtain the train timetable that can meet the passenger flow demand.

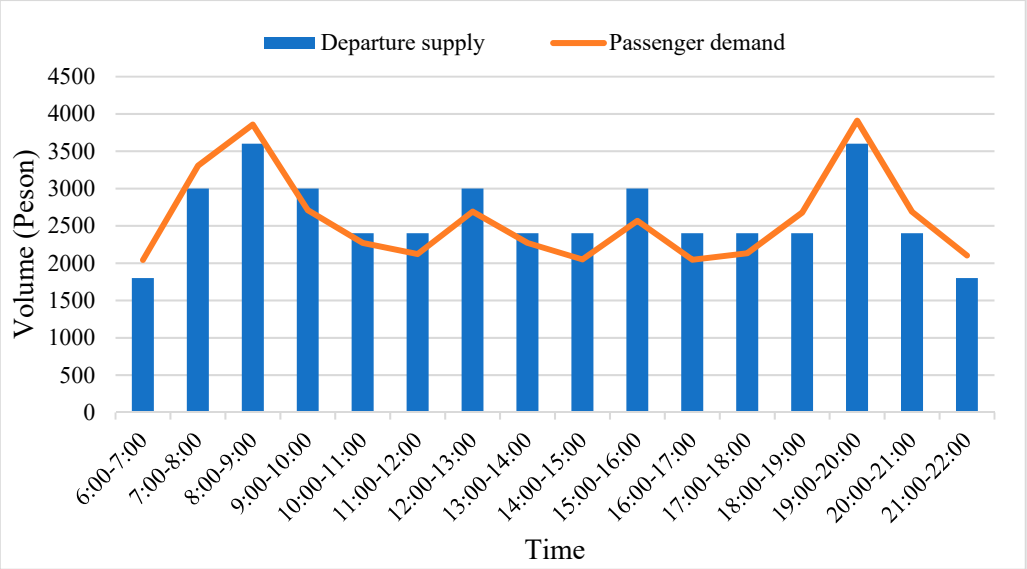

Figure 11. Supply and demand matching diagram of intercity railway.

Table 17. Details of supply and demand matching degree of multi-cycle timetable of intercity railway (6:00–14:00).

	6:00–7:00	7:00–8:00	8:00–9:00	9:00–10:00	10:00–11:00	11:00–12:00	12:00–13:00	13:00–14:00
Departure supply	1800	3000	3600	3000	2400	2400	3000	2400
Passenger demand	2043	3306	3858	2710	2272	2122	2692	2271
SDMD *	88.79%	91.16%	93.53%	89.85%	94.52%	87.72%	89.19%	94.48%

* SDMD (supply and demand matching degree): $EXP\left(-\frac{|Passenger\ demand - Departure\ supply|}{Passenger\ demand}\right) * 100\%$.

Table 18. Details of supply and demand matching degree of multi-cycle timetable of intercity railway (14:00–22:00).

	14:00–15:00	15:00–16:00	16:00–17:00	17:00–18:00	18:00–19:00	19:00–20:00	20:00–21:00	21:00–22:00
Departure supply	2400	3000	2400	2400	2400	3600	2400	1800
Passenger demand	2051	2568	2047	2133	2679	3910	2690	2103
SDMD *	84.35%	84.52%	84.16%	88.23%	90.11%	92.38%	89.78%	86.58%

* SDMD (supply and demand matching degree): $EXP\left(-\frac{|Passenger\ demand - Departure\ supply|}{Passenger\ demand}\right) * 100\%$.

Table 19 shows the performance metrics of the model for the different cases. It can be seen that compared to other timetables, the demand satisfaction rate of the multi-cycle

timetable considering the energy consumption does not decrease obviously, but the number of trains decreases significantly. From the values of the train vacancy rate, we can see that the vacancy rate of the original timetable is 24.32%, while after optimization, the vacancy rate of the multi-cycle timetable is only 6.03%, which greatly increases the operational efficiency. From the values of the total running time and energy consumption, the multi-cycle timetable performs the best. Although the multi-cycle timetable without considering the energy consumption has saved more running time compared with the original timetable, it is still inferior to the timetable where the energy consumption is considered.

Table 19. Metrics of intercity railway.

	Total Number of Trains	Demand Satisfaction Ratio	Train Vacancy Rate	Running Time (h)	Energy Consumption (kwh)
Multi-cycle timetable (with energy)	70	95.20%	6.03%	50.12	648,185.71
Original timetable	87	95.31%	24.32%	59.53	791,056.64
Single-cycle timetable	82	96.25%	18.90%	58.78	762,158.36
Multi-cycle timetable (without energy)	78	97.54%	13.60%	52.31	737,311.25

The cycle lengths of each operation line type in the multi-cycle timetable are shown in Table 20.

Table 20. Metrics of supply and demand matching of intercity railway.

Line (Line Color)	Cycle Length (min)
1 (red)	30
2 (green)	60
3 (blue)	90
4 (orange)	120
5 (violet)	660
7 (navy blue)	780
6 (purple)	660
8 (yellow green)	660

It can be seen from Figure 12 that all the trains run according to the cycle length in Table 20, and the train diagram conforms to the characteristics of the multi-cycle timetable and has a strong regularity. The multi-cycle timetable can provide a certain reference for the intercity multi-cycle train operation organization.

3.5. Discussion

By solving the multi-cycle timetable and single-cycle timetable under different passenger flow distribution scenarios, the matching degree of the supply and passenger flow demand under different distribution scenarios is analyzed. The analysis results are as follows.

For the scenario with two passenger flow peaks, compared to the single-cycle timetable, the demand satisfaction ratio of the multi-cycle timetable is 4.44% higher and the train vacancy rate is 11.49% lower. The multi-cycle timetable also saves 3.24 h running time and 15,553.6 kwh energy consumption compared to the single-cycle timetable. For the scenario with one passenger flow peak, compared to the single-cycle timetable, the demand satisfaction ratio of the multi-cycle timetable is 2.29% higher and the train vacancy rate is 9.80% lower. The multi-cycle timetable saves 2.32 h running time and 12,281.31 kwh energy consumption compared to the single-cycle timetable. For the scenario without peaks, the multi-cycle timetable could perform as well as the single-cycle timetable and saves 2.32 h running time and 13,392.31 kwh energy consumption. For the three kinds of passenger flow distributions, the passenger demand satisfaction rate of the multi-cycle timetable optimization model exceeds 98%.

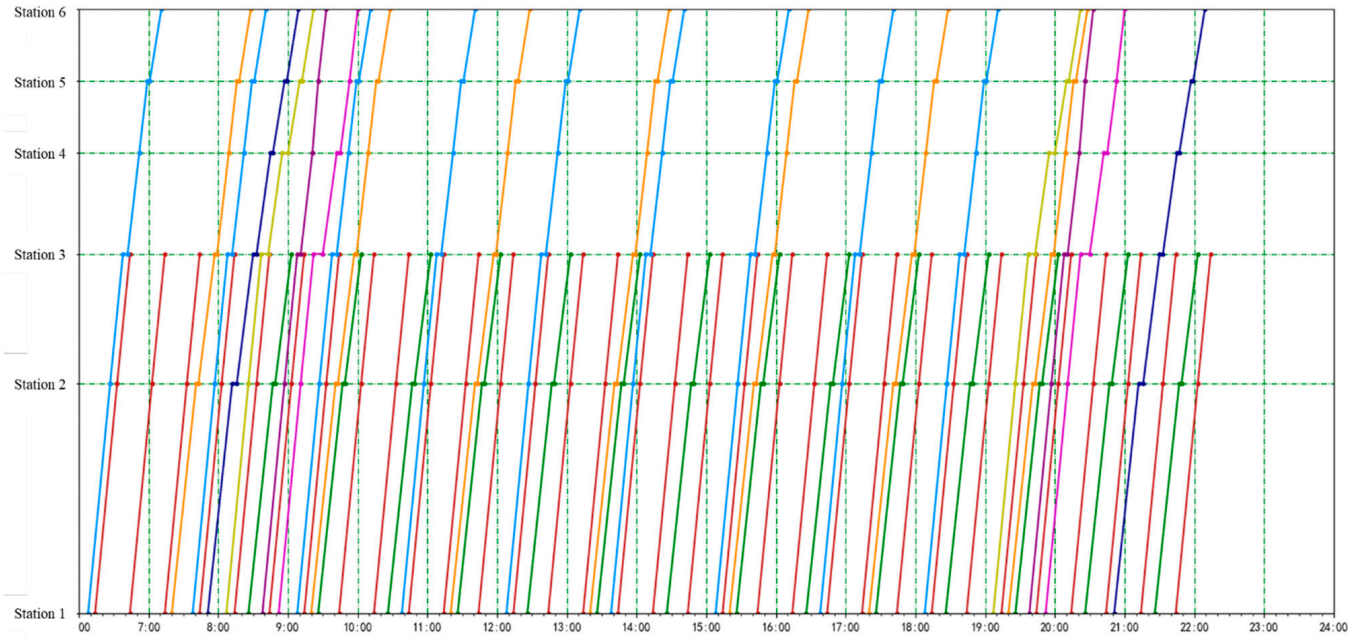

Figure 12. Multi-cycle train timetable of intercity railway. Red, green, blue, orange, violet, purple, navy blue and yellow green represents Line 1 to 8 in Table 20, respectively.

In the large-scale actual passenger flow scenario, the demand satisfaction rate of the multi-cycle timetable considering the energy consumption reaches 95.20%, and the train vacancy rate is only 6.03%, which is 18.29% lower than the train vacancy rate of the original timetable. The multi-cycle timetable considering the energy consumption saves 9.41 h train running time compared with the original timetable and saves 89,125.54 kwh energy consumption compared with the multi-cycle timetable without the energy consumption considered.

The results show that the multi-cycle timetable-compiled model proposed in this paper has a good adaptability to different passenger flow distributions. The supply of the train operation diagram obtained according to the model can change along with the passenger flow demand changes, which could ensure the periodicity of the train operation.

Compared with the single-cycle timetable, the multi-cycle timetable has strong flexibility and can flexibly adapt to various passenger flow distributions while ensuring the train running regularity. The more fluctuating the passenger flow is, the more obvious the advantage of a multi-cycle timetable is.

4. Conclusions

Providing efficient and green transportation services has always been the focus of railway expresses. As urbanization continues to expand, passenger travel demands are becoming increasingly complex, making it a challenge to optimize the supply-to-demand relationship and energy consumption jointly. Compared with the single-cycle train timetable, the multi-cycle train timetable not only ensures the regularity but also satisfies the passenger flow demand of different time periods by flexibly arranging the train departure time and the cycle length. Thus, it is necessary to develop a multi-cycle train operation that can accommodate the peaks caused by multi-source passenger demand while considering a proper combination of trains with different stopping patterns and cycles for a better energy consumption.

To this end, a multi-cycle timetable considering the supply-to-demand relationship and energy consumption (MTSDE) is proposed. The MTSDE focuses on three parts: the periodized spatial-temporal network, the optimization model and the decomposition algorithm. The periodized spatial-temporal network focuses on how to build vertex and arc sets to describe the differential operation of trains, which in turn supports the subsequent

model construction. The optimization model considers the elements of timetabling and line planning, where the elements of line planning determine the path, cycle length and stopping patterns, and the elements of timetabling determine the specific spatial-temporal points of trains. In addition, the model's objective function composes the supply demand matching degree (SDMD), the minimum time cost (MTC) and the energy consumption (EC). Based on the characteristics of the spatial-temporal network and the model, the decomposition algorithm optimizes the line planning elements and timetable elements in stages and achieves an efficient preparation of the multi-cycle complex operation diagrams by the Lagrangian relaxation algorithm. The main conclusions are as follows:

(1) The more fluctuating the passenger flow is, the more obvious the advantage of a multi-cycle timetable is. For example, if the demand has two passenger flow peaks, compared to the single-cycle timetable, the demand satisfaction ratio of the multi-cycle timetable is 4.44% higher and the train vacancy rate is 11.49% lower. The multi-cycle timetable also saves 3.24 h running time and 15,553.6 kwh energy consumption compared to the single-cycle timetable. Meanwhile, for the scenario with one passenger flow peak, compared to the single-cycle timetable, the demand satisfaction ratio of the multi-cycle timetable is 2.29% higher and the train vacancy rate is 9.80% lower. The multi-cycle timetable saves 2.32 h running time and 12,281.31 kwh energy consumption compared to the single-cycle timetable.

(2) Large-scale real cases show that this advantage still exists in practice. In a scenario, the demand satisfaction rate of the multi-cycle timetable considering the energy consumption reaches 95.20%, and the train vacancy rate is only 6.03%, which is 18.29% lower than the train vacancy rate of the original timetable. The multi-cycle timetable considering the energy consumption saves 9.41 h train running time compared with the original timetable and saves 89,125.54 kwh energy consumption compared with the multi-cycle timetable without the energy consumption considered.

Although the proposed model can make an integrated optimization for both the demand–supply satisfaction and energy consumption by an efficient algorithm, there still exists some limitations: (1) the multi-cycle timetable studied in this paper does not consider the rolling stock circulation of trains and (2) the utility of the obtained timetables in the practical scenarios was not verified. In future research, we will modify the model to integrate more practical considerations, such as the rolling stock circulation. In addition, timetables under multiple scenarios will be designed and compared to further discover the impact of seasonal and other factors on the model. The implementation of the timetables produced in this paper can be studied based on the simulation and other techniques to further optimize the model and algorithm design.

The studied methodology will support the transportation organization of rail express lines and also push the future development theme of green transportation.

Author Contributions: Data curation, H.Z.; funding acquisition, H.Z.; methodology, H.Z. and Z.H.; supervision, J.C.; writing—original draft, H.Z. and Z.H.; writing—review and editing, J.C. and J.Z. All authors have read and agreed to the published version of the manuscript.

Funding: This research was funded by the China Postdoctoral Science Foundation, grant number 2021M700186, and the China Postdoctoral Science Foundation, grant number 2021T140003.

Data Availability Statement: Not applicable.

Conflicts of Interest: The authors declare no conflict of interest.

Abbreviations

Abbreviation	Description
PESP	Periodic event scheduling problem
OD	Origin–destination
MTSDE	Multi-cycle timetable considering supply-to-demand relationship and energy consumption
SDMD	Supply–demand matching degree
MTC	Minimum time cost
EC	Energy consumption
HHLR	Hybrid heuristic Lagrangian relaxation
LB	Lower bound
UB	Upper bound
MT	Multi-cycle train timetable
ST	Single-cycle train timetable

References

1. Wang, B.; Yang, H.; Zhang, Z.H. Research on the train operation plan of the beijing-tianjin inter-city railway based on periodic train diagrams. *Tiedao Xuebao/J. China Railw. Soc.* **2007**, *29*, 8–13.
2. Serafini, P.; Ukovich, W. A mathematical model for periodic scheduling problems. *SIAM J. Discret. Math.* **1989**, *2*, 550–581. [CrossRef]
3. Peeters, L.W.P. *Cyclic Railway Timetable Optimization*; Erasmus University Rotterdam: Rotterdam, The Netherlands, 2003.
4. Cordone, R.; Redaelli, F. Optimizing the demand captured by a railway system with a regular timetable. *Transp. Res. Part B Methodol.* **2011**, *45*, 430–446. [CrossRef]
5. Goerigk, M.; Schöbel, A. Improving the modulo simplex algorithm for large-scale periodic timetabling. *Comput. Oper. Res.* **2013**, *40*, 1363–1370. [CrossRef]
6. Zhang, X.; Nie, L. Integrating capacity analysis with high-speed railway timetabling: A minimum cycle time calculation model with flexible overtaking constraints and intelligent enumeration. *Transp. Res. Part C Emerg. Technol.* **2016**, *68*, 509–531. [CrossRef]
7. Herrigel, S.; Laumanns, M.; Szabo, J.; Weidmann, U. Periodic railway timetabling with sequential decomposition in the pesp model. *J. Rail Transp. Plan. Manag.* **2018**, *8*, 167–183. [CrossRef]
8. Kinder, M. Models for Periodic Timetabling. Master's Thesis, Technische Universität Berlin, Berlin, Germany, 2008.
9. Caprara, A.; Fischetti, M.; Toth, P. Modeling and solving the train timetabling problem. *Oper. Res.* **2002**, *50*, 851–861. [CrossRef]
10. Zhang, Y.; Peng, Q.; Yao, Y.; Zhang, X.; Zhou, X. Solving cyclic train timetabling problem through model reformulation: Extended time-space network construct and alternating direction method of multipliers methods. *Transp. Res. Part B Methodol.* **2019**, *128*, 344–379. [CrossRef]
11. Odijk, M.A. A constraint generation algorithm for the construction of periodic railway timetables. *Transp. Res. Part B Methodol.* **1996**, *30*, 455–464. [CrossRef]
12. Robenek, T.; Sharif Azadeh, S.; Maknoon, Y.; Bierlaire, M. Hybrid cyclicity: Combining the benefits of cyclic and non-cyclic timetables. *Transp. Res. Part C Emerg. Technol.* **2017**, *75*, 228–253. [CrossRef]
13. Zhou, W.; Yang, X. Timetable optimization for high-speed rail with multiple operating periods: Solving method based on a framework of lagrangian relaxation decomposition. *Transp. Res. Rec.* **2016**, *2546*, 43–52. [CrossRef]
14. Zhou, W.; Tian, J.; Xue, L.; Jiang, M.; Deng, L.; Qin, J. Multi-periodic train timetabling using a period-type-based lagrangian relaxation decomposition. *Transp. Res. Part B Methodol.* **2017**, *105*, 144–173. [CrossRef]
15. Yan, F.; Goverde, R.M.P. Combined line planning and train timetabling for strongly heterogeneous railway lines with direct connections. *Transp. Res. Part B Methodol.* **2019**, *127*, 20–46. [CrossRef]
16. Niu, H.; Zhou, X.; Gao, R. Train scheduling for minimizing passenger waiting time with time-dependent demand and skip-stop patterns: Nonlinear integer programming models with linear constraints. *Transp. Res. Part B Methodol.* **2015**, *76*, 117–135. [CrossRef]
17. Nachtigall, K.; Voget, S. A genetic algorithm approach to periodic railway synchronization. *Comput. Oper. Res.* **1996**, *23*, 453–463. [CrossRef]
18. Liebchen, C. The first optimized railway timetable in practice. *Transp. Sci.* **2008**, *42*, 420–435. [CrossRef]
19. Cordeau, J.-F.; Toth, P.; Vigo, D. A survey of optimization models for train routing and scheduling. *Transp. Sci.* **1998**, *32*, 380–404. [CrossRef]
20. Yin, Y.; Li, D.; Bešinović, N.; Cao, Z. Hybrid demand-driven and cyclic timetabling considering rolling stock circulation for a bidirectional railway line. *Comput.-Aided Civ. Infrastruct. Eng.* **2019**, *34*, 164–187. [CrossRef]
21. Kim, N.s.; Van Wee, B.J.T.P. Assessment of CO_2 emissions for truck-only and rail-based intermodal freight systems in europe. *Transp. Plan. Technol.* **2009**, *32*, 313–333. [CrossRef]
22. Ritzinger, U.; Puchinger, J.; Hartl, R.F. Dynamic programming based metaheuristics for the dial-a-ride problem. *Ann. Oper. Res.* **2016**, *236*, 341–358. [CrossRef]

23. Jørgensen, M.W.; Sorenson, S.C. *Estimating Emissions from Railway Traffic*; Technical University of Denmark: Lyngby, Denmark, 1998; Volume 20, pp. 210–218.
24. Kirschstein, T.; Meisel, F. Ghg-emission models for assessing the eco-friendliness of road and rail freight transports. *Transp. Res. Part B Methodol.* **2015**, *73*, 13–33. [CrossRef]
25. Zhou, X.; Tanvir, S.; Lei, H.; Taylor, J.; Liu, B.; Rouphail, N.M.; Christopher Frey, H. Integrating a simplified emission estimation model and mesoscopic dynamic traffic simulator to efficiently evaluate emission impacts of traffic management strategies. *Transp. Res. Part D Transp. Environ.* **2015**, *37*, 123–136. [CrossRef]
26. Lindgreen, E.B.G.; Sorenson, S.C. *Simulation of Energy Consumption and Emissions from Rail Traffic*; Technical University of Denmark: Lyngby, Denmark, 2005.
27. Patterson, Z.; Ewing, G.O.; Haider, M. The potential for premium-intermodal services to reduce freight co2 emissions in the quebec city–windsor corridor. *Transp. Res. Part D Transp. Environ.* **2008**, *13*, 1–9. [CrossRef]
28. Lukaszewicz, P. Energy saving driving methods for freight trains. In Proceedings of the International Conference on Computer Aided Design, San Jose, CA, USA, 7–11 November 2004.
29. Cortés, C.E.; Vargas, L.S.; Corvalán, R.M. A simulation platform for computing energy consumption and emissions in transportation networks. *Transp. Res. Part D Transp. Environ.* **2008**, *13*, 413–427. [CrossRef]
30. Heinold, A.; Meisel, F. Emission rates of intermodal rail/road and road-only transportation in europe: A comprehensive simulation study. *Transp. Res. Part D Transp. Environ.* **2018**, *65*, 421–437. [CrossRef]
31. Wu, Q.; Spiryagin, M.; Cole, C. Train energy simulation with locomotive adhesion model. *Railw. Eng. Sci.* **2020**, *28*, 75–84. [CrossRef]
32. Chen, D.; Li, S.; Li, J.; Ni, S.; Liu, X. Optimal high-speed railway timetable by stop schedule adjustment for energy-saving. *J. Adv. Transp.* **2019**, *2019*, 4213095. [CrossRef]
33. Zhang, H.; Jia, L.; Wang, L.; Xu, X. Energy consumption optimization of train operation for railway systems: Algorithm development and real-world case study. *J. Clean. Prod.* **2019**, *214*, 1024–1037. [CrossRef]
34. Albrecht, T.; Oettich, S. A new integrated approach to dynamic schedule synchronization and energy-saving train control. *Comput. Railw. VIII* **2002**, *61*, 847–856.
35. Li, X.; Lo, H.K. Energy minimization in dynamic train scheduling and control for metro rail operations. *Transp. Res. Part B Methodol.* **2014**, *70*, 269–284. [CrossRef]
36. Lancien, D.; Fontaine, M. Computing train schedules to save energy: The mareco program. *Revue Generale Des Chemins De Fer.* **1981**, *100*, 679–692.
37. Bai, Y.; Mao, B.; Zhou, F.; Ding, Y.; Dong, C. Energy-efficient driving strategy for freight trains based on power consumption analysis. *J. Transp. Syst. Eng. Inf. Technol.* **2009**, *9*, 43–50. [CrossRef]
38. Burggraeve, S.; Bull, S.H.; Vansteenwegen, P.; Lusby, R.M. Integrating robust timetabling in line plan optimization for railway systems. *Transp. Res. Part C Emerg. Technol.* **2017**, *77*, 134–160. [CrossRef]
39. Mahmoudi, M.; Zhou, X. Finding optimal solutions for vehicle routing problem with pickup and delivery services with time windows: A dynamic programming approach based on state–space–time network representations. *Transp. Res. Part B Methodol.* **2016**, *89*, 19–42. [CrossRef]
40. Camerini, P.M.; Fratta, L.; Maffioli, F. On improving relaxation methods by modified gradient techniques. In *Nondifferentiable Optimization*; Springer: New York, NY, USA, 1975; pp. 26–34.
41. Xu, X.; Li, C.-L.; Xu, Z. Integrated train timetabling and locomotive assignment. *Transp. Res. Part B Methodol.* **2018**, *117*, 573–593. [CrossRef]